

ACCEPTED MANUSCRIPT

When X-rays alter the course of your experiments

To cite this article before publication: Wim Bras *et al* 2021 *J. Phys.: Condens. Matter* in press <https://doi.org/10.1088/1361-648X/ac1767>

Manuscript version: Accepted Manuscript

Accepted Manuscript is “the version of the article accepted for publication including all changes made as a result of the peer review process, and which may also include the addition to the article by IOP Publishing of a header, an article ID, a cover sheet and/or an ‘Accepted Manuscript’ watermark, but excluding any other editing, typesetting or other changes made by IOP Publishing and/or its licensors”

This Accepted Manuscript is © 2021 IOP Publishing Ltd.

During the embargo period (the 12 month period from the publication of the Version of Record of this article), the Accepted Manuscript is fully protected by copyright and cannot be reused or reposted elsewhere.

As the Version of Record of this article is going to be / has been published on a subscription basis, this Accepted Manuscript is available for reuse under a CC BY-NC-ND 3.0 licence after the 12 month embargo period.

After the embargo period, everyone is permitted to use copy and redistribute this article for non-commercial purposes only, provided that they adhere to all the terms of the licence <https://creativecommons.org/licenses/by-nc-nd/3.0>

Although reasonable endeavours have been taken to obtain all necessary permissions from third parties to include their copyrighted content within this article, their full citation and copyright line may not be present in this Accepted Manuscript version. Before using any content from this article, please refer to the Version of Record on IOPscience once published for full citation and copyright details, as permissions will likely be required. All third party content is fully copyright protected, unless specifically stated otherwise in the figure caption in the Version of Record.

View the [article online](#) for updates and enhancements.

When X-rays alter the course of your experiments

Wim Bras

Chemical Sciences Division Oak Ridge National Laboratory
One Bethel Valley Road, Oak Ridge TN 37831 United States
Orcid 0000-0001-5070-4039

Dean A.A. Myles

Neutron Scattering Division, Oak Ridge National Laboratory
One Bethel Valley Road, Oak Ridge TN 37831 United States
Orcid 0000-0002-7693-4964

Roberto Felici

CNR-SPIN

Area della ricerca di Tor Vergata, via del Fosso del Cavaliere 100, 00133 Roma, Italy
Orcid 0000-0001-9897-5866

This manuscript has been authored by UT-Battelle, LLC, under contract DE-AC05-00OR22725 with the US Department of Energy (DOE). The US government retains and the publisher, by accepting the article for publication, acknowledges that the US government retains a nonexclusive, paid-up, irrevocable, worldwide license to publish or reproduce the published form of this manuscript, or allow others to do so, for US government purposes. DOE will provide public access to these results of federally sponsored research in accordance with the DOE Public Access Plan

Abstract

The continuing increase in the brilliance of synchrotron radiation beamlines allows for many new and exciting experiments that were impossible before the present generation of synchrotron radiation sources came on line. However, the exposure to such intense beams also tests the limits of what samples can endure. Whilst the effects of radiation induced damage in a static experiment often can easily be recognized by changes in the diffraction or spectroscopy curves, the influence of radiation on chemical or physical processes, where one expects curves to change, is less often recognized and can be misinterpreted as a 'real' result instead of as a 'radiation influenced result'. This is especially a concern in time-resolved materials science experiments using techniques as Powder Diffraction, Small Angle Scattering and X-ray Absorption Spectroscopy. Here, the effects of radiation (5 – 50 keV) on some time-resolved processes in different types of materials and in different physical states are discussed. We show that such effects are not limited to soft matter and biology but rather can be found across the whole spectrum of materials research, over a large range of radiation doses and is not limited to very high brilliance beamlines.

Contents

Abstract	2
1. Introduction	3
2. Radiation interaction	6
2.1 Radiation absorption	6
2.2 Electron path length in matter	7
2.3 Thermal effects	8
2.4 Nature and Life time of free radicals and electronic defects in different states of matter	11
2.4.1 Soft matter	11
2.4.2 Liquids and solutions	13
2.4.3 Solid state	14
3. Interference due to radiation in structures and kinetics of processes	17
3.1 Interference in protein crystals	17
3.2 Solid State interference	18
3.2.1 Induced phase transitions	18
3.2.2 Particle growth in matrix	19
3.2.3 Electronic/conductivity effects	20
3.3 Interfaces	21
3.4 Interference with chain molecules	23
3.5 Interference and radiochemistry in water and other solvents	25

4.	Conclusions	27
5.	Acknowledgements	28
6.	References	30

1. Introduction

The main interactions of X-rays with photon energies $E = 1\text{-}50$ keV with matter result in photons being elastically/inelastically scattered or causing ionization. Inelastic scattering and photo-absorption principally produce heat, visible light or free radicals as final products. X-ray detector developers often consider this whole process and choose an interaction product that is measurable, and which can be converted to an estimate of the total number of photons that interact with the material. This is not the case when one is using an X-ray beam for scattering or spectroscopy experiments. Experimenters then in general pay attention only to the small number of X-ray photons that are scattered, or cause ionization etc., and that are relevant to their specific experimental technique. Experiments to determine material structure using techniques like (time-resolved) Small- and Wide-Angle X-ray Scattering (SAXS/WAXS), X-ray Absorption Spectroscopy (XAFS), X-ray Photo Correlation Spectroscopy (XPCS), protein crystallography etc. all expose samples to the X-ray beam for extended lengths of time. If the resulting ensemble of photon-matter interactions induce structural damage in the sample, one can often identify relative changes in diffraction peak intensities, modification in crystalline unit cells or alteration in scattering profiles etc. The damaging effects have long been known and have been extensively investigated in particular in recent years by protein crystallographers¹⁻³.

What is less expected, publicized and perhaps understood is that radiation effects can also induce phase transitions, reduction of metals, and speeding up or slowing down of chemical reactions. The unexpected interferences when samples are exposed to high X-ray dose over extended periods of time, like real time operando XAFS or diffraction/scattering experiments, has so far received much less attention and are the main subject of this overview. Here, we distinguish some more specific and sometimes unexpected radiation-induced effects that can arise, but where the presence and symptoms of radiation damage are less immediately obvious, and appear as different structures or changed reaction kinetics, compared to the same process without being exposed to X-rays

Although it might sound counter intuitive, not much attention has been given to what else happens inside a sample once an X-ray photon is counted by a detector, beyond what is required to obtain/understand for instance X-ray scattering or spectroscopy data. This measured signal, in general, only concerns a fraction of the total number of photons that interact with the sample. The rest is 'lost to the experiment' but still deposits its energy inside the sample.

The likelihood of encountering unexpected effects has increased sharply in the last decades. The increase in brilliance of synchrotron radiation sources in time is on par, or even surpasses, the increase in transistors per unit area as in the well-known Moore's 'law' (figure 1). From the bending magnets of the second-generation sources to the undulators on the multi-bend achromat rings, one has managed to

produce many orders of magnitude more photons concentrated in ever smaller beam cross sections. In combination with developments in X-ray optics and detector efficiency, this has opened up a plethora of experimental possibilities unthought only 20-30 years ago.

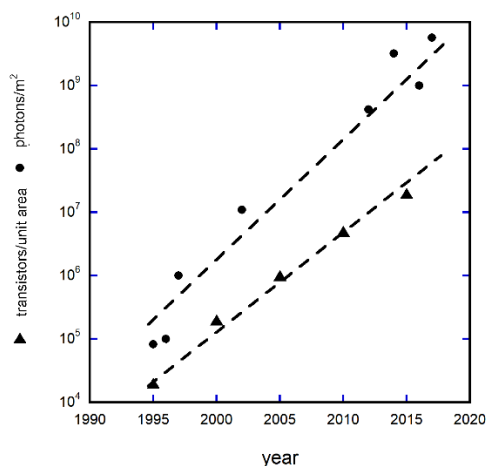


Figure 1

The increase in monochromatic flux in the last 25 years. Data obtained from beam line instrumentation publications for conventional SAXS and SAXS microfocus beam lines. The relevance is not necessarily the absolute number of photons per unit area but instead the steep increase in the number of photons deposited in a sample volume. For comparison Moore's law based on Pentium processors is shown as well. The numerical values on the vertical axis are in photons/m² as well as in transistors/unit area.

A downside of increased flux is an increasing probability of outright radiation damage, as well as for interference in for instance growth kinetics, chemical reaction kinetics or even induction of particle growth.

One of the incentives for the planned or already implemented upgrades is that with higher brilliance, data can be obtained more rapidly and therefore throughput can be increased and/or faster events can be captured and examined. For the latter, following the evolution in time of crystallizing materials or a catalysis reaction it is the physical/chemical kinetics that determine how long an experiment should last. The number of photons per time frame should be such that analyzable data is produced within the relevant time frame length. This means that for fast experiments a more intense source is required. Since radiation effects are already evident at lower X-ray doses, it will be clear that these issues become more evident with higher intensities and shorter time frames required for fast experiments¹.

We note that the new generation of X-ray laboratory sources in combination with improved optical elements, either micro source or metal-jet²⁻⁴, also allow to deposit a considerable number of photons in a small volume^{3,4}. While not as powerful as a modern synchrotron beam, they now approach the flux density of the second-generation synchrotron beam lines. The findings of effects at low photon doses therefore have clear relevance for such lab set-ups as well, increasing the number of experiments that might encounter unexpected radiation induced effects. In fact, the effects of very low radiation doses from diffraction experiments using sealed X-ray tubes already caused issues in 1959, with sucrose crystallization from lemon flavored Jell-O⁵. A very good warning that the aspect of high flux is not always the culprit but that just exposure to radiation can be sufficient.

1
2
3 We also note some comparable effects of γ -rays, IR, soft X-rays, VUV photons and electron microscopy.
4 As will be shown, any probe with an energy higher than the ionization value will result in the production
5 of a cascade of ever lower energy electrons and thus pass through the 'lower energy' range as well. The
6 prime focus is the generation of photoelectrons through the photo electric effect, which in turn may have
7 sufficient energy to create a cascade of secondary electrons.
8
9

10 Radiation damage has long been recognized. The effects on biological materials are well known and high
11 doses of radiation are even used to kill unpleasant bacteria and viruses which might contaminate food
12 stuff, sterilize medical utensils⁶ or kill fungi in museum artefacts⁷. The presence of water has also been
13 shown to have an aggravating effect. For instance, genetic damage can be inflicted by hydrolysis products
14 of radiation that interfere with DNA⁸. But even for relatively dry matter of biological origin, damage has
15 been observed and documented in for example human bones, where the hierarchical structure and
16 overall mechanical properties were altered by relatively low X-ray doses⁹. Damage is also a concern in the
17 art conservation community, which regularly uses micro computed tomography, hand held X-ray
18 fluorescence and other photoelectron spectroscopy techniques to examine organic materials, such as
19 wooden artifacts¹⁰.
20
21

22 A large body of work on radiation damage exists in the macromolecular protein crystallography
23 community, which first started to characterize the damage and subsequently devised, sometimes
24 imaginative, methods to circumvent the problems or even benefit from it by using the damage to partially
25 solve the phase problem¹¹. Surprisingly, damage effects have been much less studied, or documented, in
26 the soft condensed matter community where these effects are also well known but much less
27 documented, other than in the use of γ -rays as a tool to cross-link polymers in order to create a
28 thermosetting material¹².
29
30

31 In hard condensed matter, both for amorphous and crystalline materials, even fewer reports on radiation
32 damage induced effects exist, although specific examples such as the study of radiation induced color
33 centers are well-known¹³. Moreover, in contrast to softer materials, the radiation induced defects in hard
34 materials may be reversible and in general can be annealed by using thermal treatments¹⁴.
35
36

37 We find it interesting to note that different communities who share common concerns on radiation use
38 and effects have little interaction with each other. For instance, the lessons learned from the interaction
39 of radiation with DNA in solution in the 1960's have hardly penetrated to the biological solution scattering
40 community of today. Similarly, there appears to be a disconnect between those communities that use
41 irradiation of polymers as a crosslinking tool and soft matter scattering researchers that use X-ray
42 irradiation for characterization. Other examples of disconnect can be found, with part of the underlying
43 cause perhaps being that respective communities do not recognize that there are but few fundamental
44 differences between γ -ray, electron, soft and hard X-ray irradiation interactions with matter.
45
46

47 Although the basic concepts of the absorption of X-rays can be found in several text books¹⁵, this expertise
48 is not widely spread within the broad synchrotron radiation user community. Hence, thermal effects and
49 the production of photoelectrons, respectively the best known and most important interactions in the
50 context of this manuscript will be discussed in some detail. Throughout the current literature, except
51 perhaps for macromolecular crystallography, the reporting and discussion of radiation dose is rather
52 unsystematic with respect to the photon energy, the energy bandwidth, the irradiated volume etc. Hence,
53 we have not attempted to quantify this here. Rather, we highlight studies in which unexpected radiation
54
55
56
57
58
59
60

effects have been identified across a range of materials, and where radiation doses range from those from sealed X-ray tubes to 4th generation synchrotron radiation undulator beamlines. Obviously, the higher the intensity, the higher the probability of such effects, which is perhaps most notable in time-resolved experiments.

The text has been divided into a general section summarizing radiation interactions with matter, section 2, followed by examples, section 3, of where misleading results have been found in protein crystallography, hard condensed matter, soft condensed matter and in solutions and interfaces. Whilst protein crystallography may not be classified as materials science *per se*, we find it justified to include some of this material since in recent years radiation damage has been the most actively studied in this community. Several of the findings, and the methodology used, can be relevant for materials science as well.

2. Radiation interaction

2.1 Radiation absorption

The interaction of electromagnetic radiation with matter is a complex process and it is dependent on the photon energy and the nature of the material. This section is not intended as a comprehensive treatise on absorption, but instead to provide understanding for the large group of synchrotron radiation users whom are non-specialists in this field, of which effects are likely most relevant in the context of radiation induced sample interference. For comprehensive details there are several textbooks available^{15, 16}.

The different energy dependent absorption cross sections of processes that play a role when Iron is exposed to radiation are shown in figure 2. For synchrotron radiation-based effects, the energy range of 5 – 30 keV is most relevant and important, and here the photo-electric effect is the dominant interaction. This is similar for all other elements as well. For absorption calculations in the 50 – 30,000 eV range one can use the data from the Henke tables¹⁷. Most web-based applications are based upon these tables.

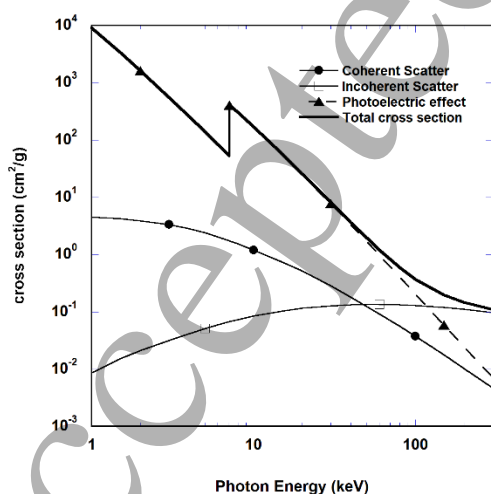


Figure 2

Cross sections for the different processes that play a role when Iron is exposed to X-rays of variable photon energy. Most materials science experiments use photons in the 5 – 30 keV range, where the photoelectric effect is dominant. (data calculated with NIST XCOM package)

An important fact to realize is that photon absorption triggers a cascade of secondary processes. The initial absorption of a photon with energy $E_{ph}=h\nu$, in the 5-30 keV range, will mainly result in the creation of a photoelectron with an energy $E_{el}=h\nu-E_0$, where E_0 is the energy level of the excited electron. The absorption cross section is maximum for electrons whose level is close, but lower, to the energy of the impinging photon. The emitted electrons have an energy high enough to create a cascade of secondary electrons²¹. There are three aspects that then require attention: (i) the distance that electrons can travel in matter; (ii) the effects of sample heating due to absorption; and (iii) the life-time of defects or excited states that have been created.

2.2 Electron path length in matter

The mean free path of electrons between inelastic scattering events in matter is energy dependent but in general below 50 nm^{18, 19}. Figure 3 shows the mean free electron path in water as a function of electron energy, which can be considered close to a universal curve valid for most matter.

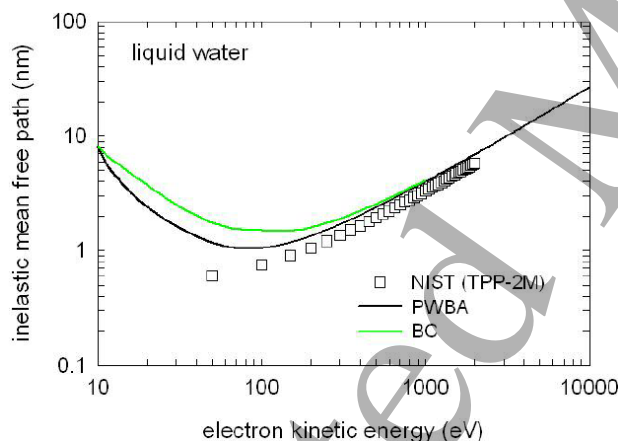


Figure 3

The calculated mean free path of electrons as function of their kinetic energy. When an inelastic collision occurs, the electron will lose some of its energy but will also change direction. The maximum pathlength might therefore be longer and consist of several segments of a random walk. Data shown for the mean free path in water. (For clarity; The different curves indicate calculations using different methodologies. The important message is that there is approximate agreement between the different methods on the free path length). Reprinted with permission¹⁹.

In the solid state, such as crystalline diamond, and with energies of up to 250 eV, this corresponds to ranges of around 0.2 nm and a lifetime of about 100 fs²⁰, increasing to 10 nm at around 1 keV²¹. However, the mean free path is not the travel range of an electron, but rather the average path length between consecutive interactions. The total path length can be calculated, using for instance the continuous slow

down approximation. For electrons of 10 keV the total path length corresponds to the order of microns. Detailed modelling studies of the interaction between high energy electrons and matter have been made²².

Since the interaction is not a single step process and a photoelectron with sufficient energy can create a cascade of secondary and higher generation electrons the aggregate volume affected by a temporary excess of free electrons will extend to several microns. A simulation of this process in a protein crystal is shown in figure 4

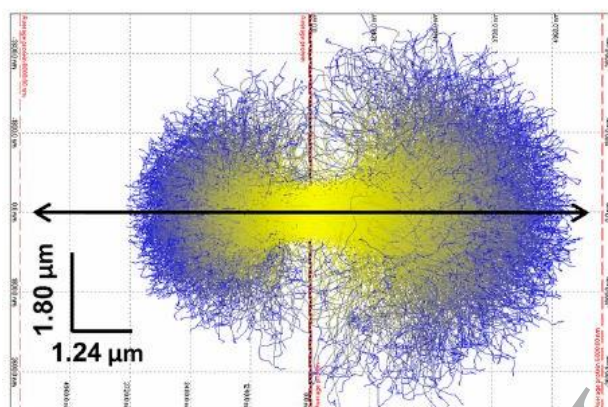


Figure 4

A simulation of the photoelectron trajectories of primary (yellow) and secondary (blue) electrons in a protein samples. Left panel for a 14.4. keV beam and right for 17.8 keV. The scale bars are indicated in the left-hand corner. This shows that the volume having a larger free electron count extends beyond the length of the mean free path between inelastic interactions. This simulation is not specific for protein crystals but can be seen as example for the general case of photo electrons in matter. Reprinted with permission²³.

The extent of the photo-electron 'cloud' and the lifetime depends on material constants and the state of matter. For micro focus beamlines, the important fact is to realize that the effects can be found even outside the direct X-ray beam.

The relevance in the context of this manuscript, is that X-ray photo absorption is a complicated and multi-step cascade process. Excess electrons will exist; for a limited time after photon absorption; in a limited volume larger than a single free photoelectron distance; in an initially increasing number but with time, reduced energy; and until they reach energy levels where they will be reduced to the source of local heating and for instance couple with phonons. Depending on the medium, radiolysis products may also exist for a longer time and will temporarily change the local environment and thus can influence time-resolved experiments.

2.3 Thermal effects

When absorbed, electromagnetic radiation will increase the temperature of materials. The questions "how much is the temperature increased" and "is this relevant for the experiment?" must then be considered.

1
2
3 The first approximation is to calculate the maximum temperature increase under the assumption that
4 there is no heat exchange between the irradiated volume and its surroundings. If that calculation causes
5 concern, one can attempt to model the temperature increase.
6

7 For the adiabatic thermal increase one can use:

$$\Delta T = A \frac{\Delta Q}{MC_p} = A \frac{NE \times 1.6 \times 10^{-16} \text{ [K]}}{V_{irr} \rho C_p \text{ [s]}} \text{ [eq 1]}$$

12 ΔT is thermal increase, A the fraction of photons absorbed by the sample, N number of photons in the
13 beam, E the photon energy (keV), V_{irr} the irradiated volume, ρ the specific mass density and C_p the
14 materials heat capacity.
15

16 A practical remark is that in real experiments, the beam is generally smaller than the sample. If a
17 temperature-controlled sample environment is used in which the thermal sensor does not measure the
18 temperature at the position where the sample intercepts the X-ray beam and hence there might be an
19 erroneous reading of the sample temperature of the material probed by the X-ray beam.
20
21

22 In modern macromolecular crystallography, to limit radiation damage effects, the sample is rapidly cooled
23 to around 100 K in order to create amorphous ice around the protein crystal. A transition from amorphous
24 to crystalline ice, which can occur around 130 - 140 K will be detrimental to the crystal. Finite element
25 modelling (FEA) on thermal effects have extensively been explored in this research community but the
26 methodology is to be considered for materials science applications as well.
27
28

29 Assuming forced cooling (FEA)²⁴, a crystal of 100 micron exposed to a 50-micron beam of 10^{15} ph/s/mm²
30 would heat the crystal by $\Delta T = 4.1 - 5.6$ K, with a temperature gradient of < 0.2 K over the total crystal
31 volume and that steady state was approached 100-400 ms after the start of the exposure. Another paper²⁵
32 also considered the same problem but now using different photon energies and crystal configurations.
33 The conclusion of these calculations is that a thin (50 μm) crystal exposed to 10^{13} ph/s/mm² would
34 increase in temperature by 6 K within 4.5 seconds, but that a thicker ($> 100 \mu\text{m}$) crystal exposed to the
35 same beam would increase 18 K over 52 seconds before reaching steady state. In view of the factor of 100
36 difference in flux the authors remarked²⁶ *The calculated temperature increase appears to be very*
37 *sensitive to the simulation parameters*. Experimental data obtained using glass balls and an imaging infra-
38 red camera showed that a maximum increase in temperature, with respect to the coolant gas temperature
39 (100 K), of 20 K occurred²⁷. Similar experiments attempted²⁸ using ruby spheres (Al_2O_3) found an increase
40 of 70 K over 25 seconds.
41
42
43

44 It is difficult to distill a comprehensive picture from such modelling and empirical methods since,
45 unfortunately, different authors include or omit different details. However, the global picture appears to
46 be that with cryo-stream cooling, it is feasible to limit the temperature increase in the sample portion
47 exposed to the direct beam to 20-40 K (authors estimate) with beams up to 10^{13} photons/s/mm².
48
49

50 In more complicated sample configurations, the modelling complexity increases. A modelling study of
51 room temperature study of gold nanoparticles²⁶ sandwiched between Kapton sheets and exposed to 6.3
52 $\times 10^{13}$ ph/s/cm² (12.4 keV photons) showed an increase of 30 K in temperature - but the measured
53 increase was just 4 K. The effects of thermal contact between the sample and a heat sink have also been
54 investigated by the thermal increase of a 100 nm diameter semiconducting InP wire. The simulations
55 showed an increase of 8 K when in contact with a heat sink and 55 K without contact, when exposed to
56
57
58
59
60

1
2
3 10¹² ph/s. When a realistic SR pulse train, instead of a continuous exposure, is simulated it is possible to
4 see thermal decay between pulses, i.e., the reaction time is very fast²⁹. Similar conclusions with respect
5 to the maximum temperature increase of Bi₂Sr₂CaCu₂O_{8+x} nanocrystals when exposed to SR pulse trains
6 were reached by using a combination of finite element analysis and Monte Carlo simulations³⁰.

7
8
9 A special case is the situation where nanoparticles with a large absorption cross section (Pb) are
10 embedded in a poor heat conducting matrix of lighter elements³¹. Here one has to take the particle size
11 and the extent of the photoelectron cloud into consideration. If the latter is larger than the particle
12 dimension most of the energy, independent of the particle absorption cross section, will be deposited in
13 the matrix. Taking dimensional considerations into account a still considerable gradient of 33K between
14 the Pb and the matrix exists at a temperature of about 600 K when exposed to a relatively low bending
15 magnet flux³¹.

16
17
18 Direct measurements of beam heating have been possible using on-line Differential Calorimeters (DSC). A
19 relatively small increase of $\Delta T = 0.2$ K was found when a Sn particle was exposed to a micro focus beam
20 (0.02 μm^2 , 15 keV, flux unknown)³². Incorporation of an on-line DSC for powder diffraction measurements
21 on an undulator beamline enabled in-beam heating to be observed and taken into account when
22 interpreting the phase transition data³³. Here there were no absolute temperatures given but instead the
23 heat flux dH/dt (mW). In diffraction experiments on PbMgNbO, Chernyshov³⁴ noted differences of 100 K
24 in sample temperature between an undulator and a bending magnet beamline, even whilst the sample
25 was actively cooled in a cryostream. This appears to be a rather extreme case.

26
27
28 As shown above both modelling as well as direct temperature measurements can also be fraught with
29 issues. A-priori knowledge of the sample's thermal behaviour without exposure to an X-ray beams is
30 therefore required to detect and distinguish heating effects. For example, in a time-resolved experiment
31 during a phase transition it was noticed that the transition occurred 8 - 10 degrees below the transition
32 temperature when compared to the controller set temperature³⁵. In another experiment³⁶, shedding light
33 on the difficult problem of beam induced thermal gradients in liquids used SAXS to observe the de-mixing
34 in a binary liquid and used the Ornstein-Zernike formalism to determine the temperature of the solution.
35 A rise of 0.45 K in the spot exposed to the direct beam of 10¹³ ph/s/mm² was observed.

36
37
38 The tentative conclusion that can be drawn from the literature is that for experiments above ambient
39 temperature and pressure, in-beam temperature increases are measurable but probably limited to
40 several degrees. This is especially true with thermally insulating samples, like polymers or ceramics, where
41 the local temperature can be some degrees off. The main issue is that when accurate temperature control
42 is required, the temperature should be measured at the position where the beam hits the sample. It is
43 also then important to verify that the temperature sensor is not also influenced by exposure to the X-ray
44 beam or to the surrounding photoelectrons that result. At cryogenic temperatures in vacuum, when using
45 a highly focused undulator, one can expect substantial thermal heating if the sample is not mounted on a
46 heat sink of some sort. The thermal read-out could be rather different from the real sample temperature.

47 48 49 50 51 52 ***2.4 Nature and Life time of free radicals and electronic defects in different states of*** 53 ***matter***

Absorbed radiation has different effects depending on the medium that absorbs it. Intuitively one can expect that effects in liquids will be much more short lived than some of those that can exist in the solid state. There are questions of mobility and life time to consider. That radiation induced excited states can exist for long times is evidenced by the fact that latent images in exposed photographic film can exist for up to 50 years and that thermal photo luminescence, due to absorbed cosmic radiation, is used to determine the age of archeological artefacts and even rocks³⁷. In daily life the self-darkening sun glasses point to reversibility and the need for continued exposure to remain in one or the other state³⁸.

2.4.1 Soft matter

Radiation processing of polymers is a common process that finds various applications, as reviewed by Makuuchi and Cheng³⁹. Schnabel explains effects in polymers exposed to both non-ionizing as well as ionizing radiation¹². In reality, the most used radiation sources are γ -rays but this is a more practical than fundamental choice. The higher penetration power allows larger objects to be irradiated with a more uniform deposition of energy. A commonly used materials parameter is the 'G value', which is defined as the 'chemical yield of radiation in number of molecules per 100 eV of absorbed radiation'³⁹ (although other definitions are also in use⁸; 1 molecule/100 eV = 1.036×10^{-7} mol J⁻¹ (or 0.1036 μ mol J⁻¹)). Values for cross linking and scission for HDPE are respectively $G_{cl} = 0.96$ and $G_{sc} = 0.48$. For isotactic polypropylene (iPP) the values are $G_{cl} = 0.2$ and $G_{sc} = 0.3$ but surprisingly for the chemically similar atactic polypropylene one finds $G_{cl} = 0.3$ and $G_{sc} = 0.45$. Values for polystyrene are < 0.02 . (see³⁹). Whatever the values are, it will be clear that each absorbed 10 keV X-ray photon can cause up to 100 events. To place this in context, an order of magnitude calculation shows that on a 10 keV, 10^{13} photons/sec, $0.1 \times 0.1 \times 0.2$ mm³ irradiated high density polyethylene (HDPE) sample, every chain of 5000 monomers sees a cross linking event every 0.02 seconds. Hence it should be no surprise that after a 10-minute exposure to a focused undulator beam the sample behaves more like a thermoset cross-linked polymer instead of showing thermoplastic behavior.

An example of a relation between the change in average molecular weight as function of radiation dose can be found¹²:

$$\frac{1}{M_{w,D}} = \frac{1}{M_{w,0}} + \left(\frac{G_{sc}}{2} - 2G_{cl} \right) \frac{D_{abs}}{N_A} \quad [\text{eq 2}]$$

Here $M_{w,D}$ is the average of the molecular weight distribution after a radiation dose D_{abs} , whilst $M_{w,0}$ is the original average. The example above is for vinyl polymers with an initial random molar mass distribution, i.e., a rather special case, but it illustrates the danger of sample modification during an experiment when one realizes that D_{abs} is a time dependent parameter.

The chemical structure of polymers has a bearing on how they respond to radiation. Methyl groups and halogens tend to increase the degradation while aromatic rings in the main chain tend to reduce the effects³⁹.

It is surprising that while most soft matter researchers using synchrotron radiation are familiar with radiation damage, there is little common literature or overlap with the community that use radiation as a tool. Most more quantitative manuscripts relate to γ - or VUV-radiation. However, to our knowledge there are few manuscripts that examine the activated sites themselves and most deal with macroscopic effects and use mechanical testing to assess how the material properties have changed. The lack of fundamental expertise is surprising since it is well known that most polymers suffer from exposure to light and there

are many manufacturers that use additives (e.g., IrganoxTM) to prolong the life time of polymers exposed to light.

In Electron Paramagnetic Resonance experiments on cross linked polyethylene exposed to γ -rays, it was found that the main issue was scission of the C-H bonds, and consequently the creation of a free radical and paired electrons that were mobile along the backbone of the polymer⁴⁰. At non-cryogenic temperatures these phenomena were all rather short lived (< minutes).

By using Electron Spin Resonance and Thermally Stimulated Luminescence on ultra-high molecular weight polyethylene (UHMWPE), polyetheretherketone (PEEK) and polycarbonateurethane (PCU) samples exposed to broadband X-rays (maximum energy 50 keV), it was found that in UHMWPE an order of magnitude more free radicals were formed than in PEEK⁴¹. These were eliminated on two different time scales. While 40% of radicals decayed within several hours, the remainder decayed to oxygen centered radicals over a period of months. In PEEK the decay time was on the order of weeks.

Using X-ray spectroscopy around the C-absorption edge (≈ 285 eV) to examine the effect on individual bonds, it was shown that the NEXAFS spectrum changed as a consequence of the radiation⁴². In such cases, a cross correlation is sometimes possible by checking if there is any mass loss in the sample, which is a clear indication of damage. However, there are cases where there is no mass loss but still a change in the NEXAFS spectrum. If one is not aware of this effect one could draw erroneous conclusions regarding the structure. See figure 5.

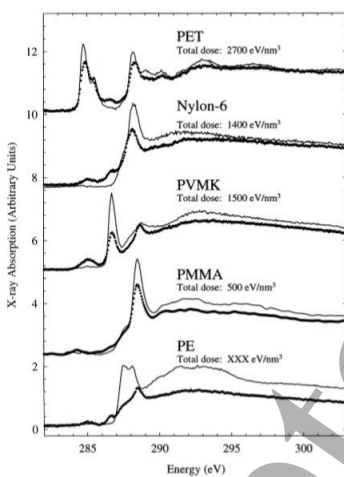


Figure 5 NEXAFS spectra from several polymers in virgin and irradiated state. By measuring the mass loss of the polymers one can perform a cross check to distinguish between radiation influence, and in this case, radiation damage. The dotted lines are the curves after exposure. Reprinted with permission⁴².

The authors of this study also showed that irradiation in the presence of atmospheric O₂ resulted in a larger amount of damage. This is probably related to the amorphous component since O₂ has more difficulty penetrating crystalline parts.

The main conclusion, based upon a limited number of manuscripts, is that the main damage caused by irradiation is the scission of C-H bonds and cross linking. There is also a variety of electronic defects, but these are temperature sensitive and do not play a large role in the processing of polymers and in general have limited life times and/or do not alter the structure much. Experiments by Goderis⁴³ have shown that

the damage can lead to changes in the glass transition temperature, which can be measured by Differential Scanning Calorimetry, though the structural evidence of which was hard to find in the SAXS patterns.

2.4.2 Liquids and solutions

Empirically, it is known that the interaction of high energy radiation with super-heated liquids can generate macroscopic effects. This is the principle of the cloud and bubble chambers, the long time work horse detectors for high energy physics research, which generated Nobel prizes for Charles Wilson (1927) and Donald Glaser (1960). These devices enable not only the primary interactions of very high energy particles to be observed, but also many other secondary high energy particles that act as sources for the nucleation of gas bubbles along their path in the liquids.

In the 1960's, Swallow produced a monograph detailing the interactions of several forms of radiation with a variety of liquids and solutions, including which intermediaries could be formed and gave estimates of their life-times⁴⁴. In 1975, Roots and Okada⁴⁵ did an exhaustive study on H₂O/DNA solutions to estimate the damage and provided a list of radiation induced solvent intermediates, their life time and their diffusion coefficients, which allows an estimate of the extent of the radiation influence around the point of photo absorption. It should be noted that this work didn't take into account the paths of the small fraction of scattered photons inside the sample, which extends the range of the interactions to a much larger volume, although with a much lower radiation product yield. While this fraction is low, it can influence the sample as will be discussed later⁴⁶. A more recent manuscript details reactions and lifetimes in a variety of solutions and in aqueous solutions at different pH values⁴⁷.

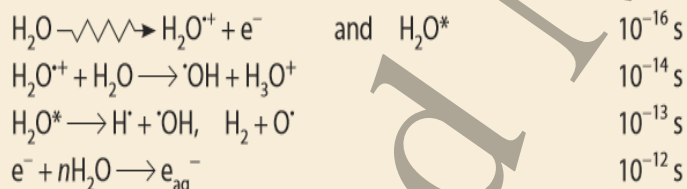


Figure 6

Radiolysis products and lifetimes. The combination of lifetime and diffusion rates determine the volume potentially affected by the radiolysis products. Data from Buxton et al⁴⁷

The principal radicals are the hydrated electron (e_{aq}^-) which is a reductant (reduction potential $E_0 = -2.87 \text{ V}$) and the hydroxyl radical ($\text{OH} \cdot$) which is an oxidant ($E_0(\text{OH} \cdot / \text{OH}^-) = 1.90 \text{ V}$ in neutral solution). In different pH regions these values change⁴⁷. The situation can be quite complex in real solutions, since different components can have differing effects on the life time of individual radiolysis radicals⁸. This is especially true in aqueous solutions, since the local chemical environment around the point of photon absorption can temporarily be changed, generating for instance changes in pH which can last up to 4 ms and diffuse over a distance of 4 μm around the point of absorption. With a high enough flux, chemical reactions inside the beam might therefore show different kinetics or be inhibited⁴⁸. Electron/liquid interactions are also important in environmental electron microscopy cells⁴⁹⁻⁵¹ and it is likely that there are similarities in the observed phenomena.

1
2
3 It is perhaps ironic to note that while some research groups use radiolysis products to create nanoparticles
4 in solution^{52, 53}, others use very intense X-ray beams to follow the kinetics of the formation of
5 nanoparticles in solution scattering experiments. A brief survey on the application of radiation to form
6 nanoparticles reveals that in the case of organics, cross linking is the main driving force, whilst in the case
7 of inorganic nanoparticles the change of chemical environments and the creation of free radicals will drive
8 particle formation⁵⁴. Apart from the direct effects of the radiation itself, it is also possible that the
9 presence of a solid/liquid interface plays a role. An example where a synchrotron beam was used to induce
10 particle formation without being the experimental probe beam uses this solid/liquid interface⁵⁵. The
11 particles were subsequently analyzed by SEM etc. Although the authors don't provide an exact dose
12 estimate it could be noted that these irradiations were performed on a superbend magnet beamline with
13 a critical energy of around 3 keV using a polychromatic beam (1 – 20 keV). Depending on the photon beam
14 size the photo-electron production rate is comparable to a monochromatic undulator beamline.

15
16
17
18 Further information on radiolysis products in a variety of hydro carbons and chlorinated hydrocarbons⁴⁷
19 and on reaction products and reaction rate constants for both polymers as well as bio-based polymers
20 can be found in a monograph by Schnabel¹².

21 22 23 24 25 **2.4.3 Solid state**

26
27 The solid state is a huge category where one intuitively feels that there will be a difference between
28 amorphous and crystalline solids. Moreover, due to the prominent role of photoelectrons in radiation
29 absorption events, it is safe to assume that there will be a difference between conductors and insulators.
30 Therefore, while we outline some of the basic effects involved, we concentrate on examples where
31 radiation products that are the most plausible to influence time-resolved experiments.



45
46 *Figure 7*

47
48 *The glass vacuum window of a synchrotron beamline monochromator vessel. The shadows of the Venetian*
49 *blind where less of the radiation has hit the window, on the inside of the vacuum vessel is clearly visible.*
50 *The more exposed areas have turned brown due to the formation of color centers. The radiation source*
51 *here is the scattered radiation in the vessel, not any direct beam. Experience tells that a moderate heat*
52 *treatment will restore the glass to its normal transparent state, indicating that the cause of the browning*
53 *are metastable electronic defects. (Photograph courtesy of Dirk Detollenaere)*

1
2
3 Within the energy range we discuss, photons and photoelectrons do not have sufficient energy to cause
4 a cascade of atomic displacements via direct collisions^{56, 57} (In some parts of the literature this is named
5 'knock-on damage'). This is unlikely to occur with (photo)electron energies below 60 keV⁵⁸. The maximum
6 direct influence on a crystalline structure will be the formation of a Frenkel pair, i.e., an interstitial-hole
7 combination with a displacement threshold of approximately 10-50 eV⁵⁹. Local damage can be very stable
8 and when only a small amount is present, might have some effect on material parameters but in X-ray
9 experiments might only be discernible as a slight broadening of diffraction peaks. In the realm of electron
10 and ion beam damage studies the formation of a Frenkel pair is, confusingly, called 'radiolysis' which in
11 the chemistry domain is terminology reserved for the dissociation of molecules. It is interesting to note
12 that in periodic structures like semi-conductors and metals, atomic displacements can take place even at
13 lower electron energies. This is attributed to damage effects combining and causing local 'Coulomb
14 explosions', and a combination of the presence of excited states with ballistic electron energy transfer<sup>56,
15 57, 60</sup>. This indicates that very high doses of radiation could locally have a cumulative effect and create
16 issues which one normally would only associate with higher energy electrons.
17
18
19

20
21 Besides the direct displacement of atoms, the change of chemical states can affect the local structure of
22 a crystal or amorphous material. Upon photon absorption electrons can be excited from the valence to
23 the conduction band, creating a hole in the valence band. Such electron hole pairs can recombine rapidly
24 but the possibility also exists that they are trapped at existing or newly created defect sites and have an
25 extended to infinite life time⁶¹. A distinction is sometimes made between intrinsic and extrinsic defects
26 where the intrinsic defects are associated with 'defects' in the glass structure and extrinsic refers to the
27 photo ionization of dopants⁶². A characteristic is that these effects are all temperature sensitive and can
28 be removed by annealing samples at a higher temperature or by using laser bleaching. This indicates that
29 for time-resolved experiments at elevated temperatures the possibility that these defects will play a role
30 is not very high.
31
32

33
34 The nature of defects in crystalline materials that can be created upon irradiating with X-rays is illustrated
35 by an experiment where a KD_2PO_4 crystal was irradiated with polychromatic X-rays (maximum 60 keV)
36 whilst the sample was held at 77K. Several defects structures are known and associated with vacancies
37 and holes in the KD_2PO_4 crystalline lattice⁶³. By slowly raising the temperature. Electron Paramagnetic
38 Resonance (EPR) and optical measurements showed that all these excited states annealed out and would
39 have a very short life time at room temperature and above.
40

41
42 The longer-term stability of X-ray induced color centers in silver doped glasses has also been investigated.
43 In this case, for samples stored in the dark but otherwise kept at ambient conditions, spontaneous decay
44 was found to extend over a period of up to two years⁶⁴.
45

46
47 In a comparative study of recent as well as fossilized teeth, samples from both human and animal origin
48 exposed to monochromatic photons (10^{11} ph/s/mm²) showed distinct discoloration⁶⁵. While the variability
49 between the species was considerable, a common factor was that upon exposure to ambient UV light, the
50 samples bleached considerably. However, some samples retained a permanent discoloration even after
51 24 hours exposure of high intensity artificial UV light. It is not clear if this permanent discoloration is due
52 to organic material in the teeth. The interesting point of this experiment was that the total dose didn't
53 show a clear correlation with the degree of coloration, nor with the photon energy, indicating that
54 somehow it is possible to reach a saturation level.
55
56
57
58
59
60

1
2
3 The life time of color centers in amorphous materials probably has several time constants and these will
4 be temperature dependent as well. The anecdotal experience of the browning of vacuum windows in high
5 radiation environments which will persist for years indicates already a nearly infinite life time component.
6 Studies on borate glasses⁶⁶ showed that color centers persist for many hours at ambient temperature, but
7 for just 10's of minutes at 70 °C illustrating the temperature dependence and transient nature at elevated
8 temperatures. In contrast the well-known photochromic glasses, already discovered in the late 1930's,
9 have reversible darkening and lightening times on the order of seconds³⁸.

10
11
12 In metal containing proteins the photoelectrons can reduce the metal center and change the first
13 surrounding shell⁶⁷. These changes have been investigated by pulsed radiolysis and by XANES
14 measurements on Mn containing centers⁶⁸. For the latter method, one obviously has to be aware that the
15 probe photons can change the electronic state of the Mn during the experiment.

16
17
18 Reduction of Ag²⁺ due to either UV or γ -irradiation in Zn and phosphate glasses has been investigated by
19 EPR⁶⁹. In the case of exposure to a UV laser, the formation of Ag clusters was attributed to the local heating
20 and increased mobility of the Ag atoms, which are not mobile at ambient conditions. In contrast, γ -
21 irradiation did not show the clustering but only the formation of Ag⁰, which was deemed to be stable at
22 ambient temperature.

23
24
25 The above examples show the broad range of defects and lifetimes that can occur. The research field of
26 radiation induced in solids is that large that a full journal is dedicated to this (Radiation Effects and Defects
27 in Solids, Wiley).

28
29
30 Generally, unless a very high dose of X-rays is used, structural changes remain limited to the creation of
31 interstitial-hole Frenkel pairs and that excited electronic states can persist over a very large range of times,
32 but that none of these effects has an extended life time at elevated temperatures.

33
34
35 What the effect of the presence of photoelectrons may be in catalysis, often the meeting point between
36 solid-liquid or solid-gas systems, has not yet been investigated in depth. Anecdotal stories about increased
37 reaction rates exist, but whether this is due to the presence of photoelectrons; or temporary valence
38 changes in the catalytic active sites of the metallic particles; or the interaction between the catalyst carrier
39 and the catalytic active particles, is not clear. What is clear is that materials with excited states can behave
40 chemically rather different compared to the native state. Abundant evidence of this lies in the chemical
41 development of photographic films and paper where the interaction of silver halogenides with a
42 developer like hydroquinone reduces the activated silver halogenides to elemental silver faster than the
43 non-activated material⁷⁰. A process that was, and still is, used over a century after its invention.

44 45 **3. Interference due to radiation in structures and kinetics of** 46 **processes**

47 48 49 **3.1 Interference in protein crystals**

50
51
52
53 Although radiation damage and deterioration in protein crystals has been studied extensively^{11, 23, 71-75} less
54 attention has been given to radiation effects that do not destroy the crystals but change them. This is
55 especially the case in redox-active metalloproteins where the redox state of the active center can be
56
57
58
59
60

1
2
3 changed by irradiation, and thus can lead to erroneous interpretations of their catalytic activity. This is
4 unlikely to be specific for protein crystals but can act as a model for inorganic crystals as well.
5

6 Many proteins rely upon high-valent 3d transition-metal ions (such as copper or iron) for function, where
7 the oxidation and coordination state of the metal determines the redox properties and molecular
8 interactions of the protein⁷⁶. Such metal centers are prone to photoreduction, whereby photo-electrons
9 reduce the high-valent active metal site(s), thereby altering their electronic structure and bonding
10 interactions. These electrons are still mobile at the cryogenic temperatures where most protein diffraction
11 experiments are carried out and propagate rapidly to electrophilic centers⁷⁷. The formation rate of
12 photoelectrons is fast (10's of fs) and these X-ray induced effects accumulate rapidly (on the seconds to
13 minutes long duration of a typical X-ray data collection), and can give rise to mixed redox and structural
14 states that complicate interpretation of the underlying chemistry. Thus, in addition to being subject to
15 the same radiation induced issues of local chemical modification and global changes that limit diffraction,
16 analysis can be directly impacted and compromised by X-ray driven changes in the valence and oxidation
17 state of the metal centers.
18
19
20

21 Such X-ray induced effects are manifold in heme^{78, 79} and copper⁷⁷ containing metallo-proteins, not even
22 more exemplified in studies of photosystem II (PS-II), a key component of the photosynthetic apparatus.
23 Light captured by the reaction center drives water oxidation and oxygen generation through a bound
24 Mn_4CaO_5 cluster that forms the redox center of the oxygen-evolving complex (OEC)⁸⁰ The redox chemistry
25 is complex, involving cycling through five intermediate S-states (S0-S4s)⁸¹ – and unravelling the structural
26 basis of the O-O bond formation though the cycle presents a particular challenge. Complicating this, PS-II
27 is very radiation sensitive and X-ray induced photoreduction of Mn ions in the OEC has significantly
28 complicated interpretation of the mechanism involved^{68, 82-84}. Specifically, X-ray induced reduction of the
29 OEC Mn(III) and Mn(IV) ions to Mn (II) by solvated electrons has been shown to disrupt the bridged
30 Mn_4CaO_5 structure, breaking the Mn di- μ -oxo units, and giving rise to a mixture of metal bound sub-states
31 in the resulting X-ray crystal structures.
32
33
34

35 While these X-ray photoreduction effects are essentially unescapable, they can also be harnessed in
36 experiments designed to use X-rays to control and drive redox reactions within the crystals. An early,
37 striking example of this approach used X-rays at different wavelengths (0.9 and 1.4 Å) to capture
38 intermediate states of the heme iron-oxygen complex in the hydroxylation reaction of camphor by
39 P450cam⁸⁵. As another example; X-ray-induced photoreduction enabled a catalytically relevant Michaelis
40 complex structure of ferrous aldoxime dehydratase to be captured from crystals of the inactive ferric
41 aldoxime complex⁸⁶.
42
43
44
45
46
47
48

49 **3.2 Solid State interference**

50
51 Photographic materials, silver halogenides embedded in gelatin and deposited on a plastic film, have
52 played an enormous role in the 20th century. It is rather ironic that only near the tail end of the mass use
53 of this technology one has developed tools that can show in real time what actually happens in the AgBr
54 grains when exposed to radiation. In this case the X-ray beam is both the irradiation tool as well as the
55
56
57
58
59
60

1
2
3 probe beam, for XRD, used for the experiment. The photo chemistry of AgBr is well known. $\text{Br}^- + h\nu \rightarrow \text{Br}^- + e^-$ and $e^- + \text{Ag}^+ \rightarrow \text{Ag}^0$. On the nanoscale this has as consequence that the AgBr lattice will distort due to
4 + e^- and $e^- + \text{Ag}^+ \rightarrow \text{Ag}^0$. On the nanoscale this has as consequence that the AgBr lattice will distort due to
5 the buildup of Ag crystalline regions. The resulting stress will cause the AgBr crystalline grains to break up
6 in several smaller grains which can rotate due to the stress relaxation taking place⁸⁷. The time scale with
7 which this occurs is on the order of 10 - 30 seconds. The authors showed that this is a mechanical effect
8 taking place due to the photo chemistry, since under similar conditions Ce and Ti oxide particles did not
9 show this kind of behavior.
10
11

12 **3.2.1 Induced phase transitions**

13
14
15 Although photo induced structural changes at cryogenic temperatures are somewhat counter intuitive,
16 they have been observed in YBaFe_4O_7 crystals⁸⁸. The stable phase below 190 K is monoclinic but when
17 irradiated at 4 K with 20 or 30 keV photons a phase transition to the stable tetragonal phase (for $T > 190$
18 K), is observed. This tetragonal phase remains stable, even in the absence of X-rays, till the temperature
19 is increased. The authors make a case that the X-rays destroy the charge ordering between Fe^{2+} and Fe^{3+}
20 species, thus creating an electronic cascade which stabilizes a hole in the core levels and which requires a
21 change in the Fe-O bond, thus inducing the phase transition.
22
23

24 The radiation induced transformation of the amorphous to the crystalline state has been observed in
25 several glassy as well as metallic systems. What should be emphasized here is that this apparently can
26 occur over a wide range of radiation doses. For example, the changes that occur when amorphous Si is
27 exposed to a low energy electron beam is sufficient to induce crystallization^{89, 90}. Here the explanation is
28 that dangling bonds, or free radicals, become mobile and find a lower energy state which is closer to the
29 crystalline state. There appears to be a similarity between thermal treatments and exposure to radiation
30 in this case. Such a link between thermal and radiation induced crystallization appears to be missing in
31 another example where a mechanically buckled BaTiO film was exposed to an intense undulator beam (12
32 $\times 12 \mu\text{m}^2$, 10^{10} ph/sec, $E = 24$ keV). The authors here provide as a possible mechanism a significant growth
33 in atomic vibrational amplitudes which can lead to the displacement of light atoms and which ultimately
34 can lead to stress relief of the mechanically stressed films⁹¹.
35
36
37

38 A combination of high temperature and radiation can cause crystallization in Lithium Disilicate to occur at
39 a much lower radiation dose than in the previous examples⁴⁶. Even the influence of scattered radiation
40 was sufficient to induce and accelerate crystallization. The proposed mechanism is that the
41 photoelectrons interfere with the dangling bonds which are present in the original glass matrix. These
42 experiments were carried out on a medium intensity bending magnet beamline ($300 \times 1000 \mu\text{m}^2$, 10^{11}
43 ph/sec, $E = 10$ keV). It should be remarked that the radiation dose due to scattered radiation is many
44 orders of magnitude lower (10^6 - 10^7 estimate) that in the direct exposure to an electron beam or a focused
45 undulator beam. This highlights again that, unfortunately, trying to create a general overview of dose
46 dependency is futile and that this has to be assessed for every class of samples separately.
47
48
49

50 **3.2.2 Particle growth in matrix**

51
52
53 Exposure to X-rays has been observed to create metallic nanoparticles in metal doped materials. The
54 similarity between the luminescence of Ag particles formed by exposure to very high doses of soft X-rays
55 ($E = 3.542$ keV, dose not clear) at ambient temperature and those obtained by a heat treatment of a nano-
56
57
58
59
60

porous zeolite has been reported⁹². In most cases the heat treatment allows the metal ions to become mobile, which enables a random walk of the atoms through the lattice. This is not feasible at ambient temperature and hence the effect must be due to knock-on effects that create Frenkel pairs and do not allow large clusters to grow. This implies that a very high radiation dose as well as a high degree of doping is required in this specific case. However, the authors concentrate on the luminescence effects and do not provide a theory for the cluster formation at room temperature.

In a study that mainly focused on the luminescence a sulfophosphate glass doped with Ag and Ce, an increase in SAXS intensity was reported as function of exposure to several hours of UV radiation⁹³. Since these irradiations were carried out at ambient temperature, it is somewhat surprising that the authors attribute the SAXS patterns to electron density fluctuations with a diameter of about 15 nm. Subsequent thermal treatments did not produce further changes in the SAXS patterns, i.e., it is clear that a structural change had occurred but if this is due to Ag particle cluster formation is maybe debatable. It is known that the doping with Ce lowers the threshold for reduction of Ag^+ to Ag^0 and it is also known that Ag can be mobile in glass at low temperatures⁹⁴. Hence, while Ag cluster formation upon UV or X-ray irradiation might be surprising, but indeed may be feasible^{62, 93}.

The opposite case, where an existing gold metallic cluster was reduced in size, has also been reported following a combination of exposure of Au doped silicate glasses to a synchrotron radiation beam of 32 keV, 10^{12} photons $\text{mm}^{-2}\text{s}^{-2}$, and subsequent thermal treatment⁹⁵.

Gold particle growth in soda lime silicate glass was studied by in-situ SAXS measurements whilst the samples were kept at elevated temperatures, allowing Au mobility. The X-rays here serve the dual function of experimental probe beam and photoelectron source⁹⁶. It was found that the growth of the particles was initially accelerated due to the exposure to X-rays, but when compared to ex-situ heated samples the onset of Ostwald ripening, i.e., the growth of larger clusters at the expense of smaller ones, was delayed. These effects are attributed to the reduction of Au^+ to Au^0 which enhances the diffusion coefficient. It is in fact only due to that fact that the authors compared in- and ex-situ results that the differences in growth rate due to radiation were noticed.

An even more direct proof of the interference of radiation with particle growth can be found in a SAXS experiment on the thermally induced growth of PbS particles in a borosilicate glass matrix by Stanley³¹. Inside this matrix, lead occurs either as the mobile Pb^{2+} or as immobilized Pb^{4+} in the glass network. Due to the preparation method, there was excess Pb in the sample. In both the irradiated and non-irradiated parts of the sample, PbS quantum dots formed at elevated temperatures. However, in the irradiated part of the sample, growth of metallic Pb particles was also observed. Initially highly monodisperse, when the Pb was depleted Ostwald ripening occurred. It is striking that these cubic Pb crystals formed only in the region exposed to radiation.

3.2.3 Electronic/conductivity effects

Current generation due to absorbed X-rays has been used as a tool to characterize single nanowire solar cells⁹⁷. See figure 8. For this, a nano-focus X-ray beam was aimed at such a solar cell in order to measure the spatial variations in the charge collection probability. Whereas many experimenters do not take creation electron-hole pairs into account when assessing the effects that radiation may have on their samples, these experimenters effectively harnessed this current as a tool.

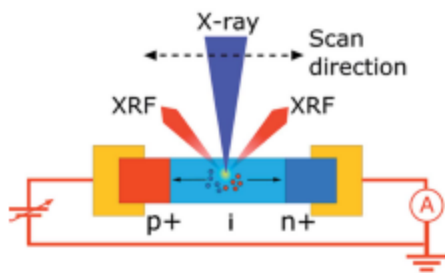


Figure 8

Experimental lay-out for the experiments described above. A nano focus beam with a cross section of $50 \times 60 \text{ nm}^2$ and a photon energy of 17 keV was used to positionally scan the sample. At each position the induced current was measured. Reprinted with permission⁹⁷.

That the conductivity of materials can be influenced by exposure to radiation is well known in semiconductor and photovoltaic research and industries but less well studied in other materials. A phase transition in an antiferromagnetic manganese oxide insulator irradiated at $T < 40 \text{ K}$ has been observed to change to a metallic ferro magnetic state when exposed to X-rays⁹⁸. Neutron diffraction showed a doubling of the crystalline unit cell. This conducting state persisted after irradiation was stopped but was sensitive to thermal cycling and high magnetic fields. The authors assume that the effect was due to photoelectron interaction with the samples. In a later paper, the conductivity is suggested to be due to electron tunneling between metallic islands⁹⁹.

The thin MoO_3 films used in solar cells undergo a reduction from Mo^{4+} to Mo^{5+} when exposed to 1.2 keV photons, even at relatively low doses, which the authors attributed to Oxygen vacancies created by irradiation¹⁰⁰. This can clearly be seen as a case of radiation induced damage, but when studying the performance of the solar cells, these damage effects can easily be convoluted with other damage effects. The role that these layers have in solar cells as electronic hole extraction layers means that any damage will have an effect on the performance of the cell.

In $\text{Pt}/\text{TiO}_2/\text{Pt}$ cells, where a 40 nm TiO_2 layer is sandwiched between two platinum slabs with a bias of 0.2 V , a multitude of effects can be found as function of both beam intensity as well as exposure time¹⁰¹. For short exposures, an induced current four orders of magnitude above the base level was observed (beam parameters 8.3 keV , $2 \times 10^{13} \text{ photons}/(\text{mm}^2\text{s})$). However, for exposures up to 24 hours, the current increased by several orders of magnitude and persisted even after cessation of irradiation. The low dose behavior can be explained since TiO_2 is a well-known photocatalyst. The authors appear to neglect the fact that the TiO_2 layer of 40 nm is thinner than the range of the induced electron avalanche, which might explain an increase in the current. The increase of current after long exposures is attributed to defect formation and induced phase transition.

By using a very high X-ray dose (17 keV , $2 \times 10^{11} \text{ photons}/\text{sec}$ in $1.3 \times 10^{-2} \text{ mm}^2$) it has shown to be possible to change the critical temperature for superconductivity, T_c , in a $\text{Bi}_2\text{Sr}_2\text{CaCu}_2\text{O}_{8+\delta}$ ($\text{Bi}2212$) superconductor¹⁰². An elongation of one of the crystalline axes was explained as a consequence of radiation induced change of O-content. Here, the O atoms are being displaced by the knock-on effect of secondary electrons. It should be noted that the dimensions of the elongated crystals were less than the expected extent of the photoelectron and secondary electron cloud. Hence to calculate a real dose

1
2
3 dependence would be complicated. It should be pointed out that this effect could also be classified as
4 radiation damage but since the change in T_c takes place gradually and the elongation of the crystalline
5 unit cell is rather difficult to observe
6

7 In glasses, events around the glass transition temperature do not show up as structural changes. However,
8 the structural relaxations, or microscopic motion, as probed by XPCS measurements, are considerably
9 faster when exposed to high doses of X-rays^{103, 104}. The authors observe that the magnitude of these
10 effects are beam intensity dependent and appear well below the energy levels required for atomic knock-
11 on effects¹⁰⁴. Attempts to distinguish between the natural glass dynamics and the beam induced dynamics
12 rely on computational methods with, obviously, the complications involved in such an approach¹⁰³. It is
13 also interesting to note that this effect is observed in oxide glasses but not in metallic glasses.
14
15

16 Radiation induced chemical reactions rates in solids have been discussed in a monograph on reaction
17 kinetics¹⁰⁵.
18

19 **3.3 Interfaces**

20
21
22

23 The issue of radiation interference at interfaces is even more complicated, since one is dealing with solid-
24 liquid or solid/gas combinations where the radiation can have effects on both media. This is especially
25 relevant in operando catalysis studies. X-ray spectroscopy techniques like EXAFS and XANES often require
26 extended exposure due to variations in catalyst gas loading and repeated reaction cycles. A systematic
27 study, dealing not with structural or electronic defects but instead focusing on the relation between X-ray
28 dose and the conversion rate of methane to methanol by a Cu catalyst has indeed shown a significant
29 effect¹⁰⁶. The working hypothesis is that the radiation reduces Cu^{2+} to Cu^+ and that this has a negative
30 effect on the conversion rate of the methane. To paraphrase the authors: 'The comparative results
31 obtained from this study show that a considerable misrepresentation of the behavior of the Cu catalyst
32 at numerous levels may be arrived at when using a high intensity focused X-ray beam'. Noteworthy is that
33 these effects were not radiation dose dependent but were already present from the start of the
34 experiment. To avoid issues as experienced on high intensity beamlines (10^{12} - 10^{14} photons/(mm²sec), the
35 incident beam intensity had to be reduced by a factor of around 1000 using amorphous carbon filters. The
36 unfortunate truth in this case is that the beam intensity was attenuated back to the level of bending
37 magnets at third generation synchrotrons, before any upgrades.
38
39
40

41 The above study focuses on the effect of radiation on the metallic particles and leaves unanswered the
42 question of whether the photoelectrons could interfere in the catalytic process itself. For this, we only
43 have anecdotal evidence in that in some cases the catalytic reactions on the beamline proceeded much
44 faster than in the home laboratories^{48, 107}.
45
46

47 That photon absorption can lead to interference in catalytic processes was also found when a white beam
48 was used to enhance the electrolytic deposition of Ni-P alloys from solution. This process is pH sensitive
49 and autocatalytic, and takes place regardless of the presence of X-rays. However, exposure to X-rays
50 speeds up the process considerably and has similar effect to increasing the pH¹⁰⁸. This could indicate an
51 increase in the pH due to irradiation, but the authors also provide evidence of another pathway through
52 which X-rays generate hydrogen radicals that then help to reduce the Ni ions. This would imply two
53 parallel processes with similar result. Similar experiments were reported for the deposition at room
54 temperature of Cu layers from solution^{48, 55, 109-111}. The formation of metallic particles, however, is not
55
56
57
58
59
60

1
2
3 limited to white beam irradiation and focused monochromatic undulator beams have also been shown to
4 affect the growth kinetics of Au particles from solution at lower intensity beamlines¹¹².
5

6 A modification of the surface due to desorption of oxygen from a Pt surface covered with a thin water
7 layer has been reported and is attributed to the radiolytic water products enabling the desorption
8 process¹¹³. In a control experiment, in a high vacuum environment, this effect was not observed.
9

10 To our knowledge, no systematic study has yet been performed to examine the effect of the directionality
11 of the X-ray beam, i.e., at right angles or parallel to the interface. One can imagine that when the X-ray
12 beam is orthogonal to the interface, there will be a gradient of photoelectrons in the solvent layer which
13 might be relevant in coating studies.
14
15

16 A combination of X-ray scattering, imaging and modelling was used to examine radiation effects on a
17 calcite-water interface¹¹⁴. Here the equilibrium dissolution rate was enhanced due to exposure to 10 keV
18 photons from a focused undulator beam. The dissolution rate at steady state was observed to be 2.2
19 monolayers/sec, in close agreement with modelling where the assumption was that the radiolysis
20 products caused an acidification from pH = 8.3 → 5.2. There was a marked difference between the initial
21 stages and steady state. In light of the many bio-crystallization studies performed in the last decade, this
22 is the first somewhat more quantified results that takes the effect of radiation into account and indicates
23 that such pH dependent results have to be approached with caution and the lowest radiation dose and
24 larger beam dimensions should be used.
25
26

27 The water-air interface is also not immune to radiation influence. In an experiment in a closed capillary, it
28 was shown that the evaporation rate of H₂O increased due to exposure to radiation. Both thermal effects
29 as well as chemical hydrolysis reactions, e.g., gas formation, could be ruled out and the authors explain
30 the increased evaporation rate as being due to changes in the surface tension¹¹⁵, even though no changes
31 in the shape of the meniscus were observed. The radiation dose in this case was expressed in the number
32 of ph/Å² and was calculated to be 0.1 ph/Å² (13 keV), well below the limit of 200 ph/Å² were the authors
33 claim Coulomb explosions can occur.
34
35

36 **3.4 Interference with chain molecules**

37
38

39 The glass transition temperature, T_g , is an important parameter in polymer physics and is related to the
40 polymer molecular weight via the Flory-Fox relation:
41
42

$$43 T_g = T_{g,\infty} - \frac{K}{M_w} \text{ [eq 3]}
44$$

45 The effects of ionizing radiation on long chain molecules are a combination of chain scission and cross
46 linking. Whilst chain scission will reduce the average molecular weight, M_w , which in turn will decrease
47 the glass transition temperature, cross linking will increase this. Figure 9 shows the schematic
48 development of the M_w as function of radiation doses in the different scenarios. The numerical values are
49 different for each polymer and have to be determined empirically. The parameters $G(x)$ and $G(s)$ have
50 been defined before in this text.
51
52
53
54
55
56
57
58
59
60

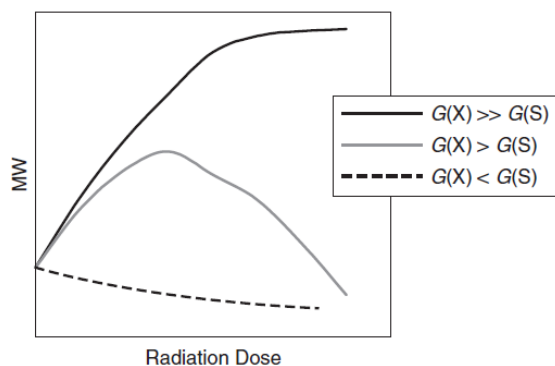


Figure 9

Schematic description of the M_w dependence as function of radiation dose for different efficiencies of cross-linking $G(x)$ and scission $G(S)$. These parameters have to be empirically determined for every polymer and can vary by an order of magnitude between polymers. The underlying effects, however, are for every polymer the same. Figure from Makuuchi and Cheng³⁹

As previously mentioned, Goderis⁴³ has examined the effects of the radiation dose using Differential Scanning Calorimetry (DSC). A systematic study on polymethylmethacrylate (PMMA) using monochromatic X-rays showed a decrease of the T_g from 119 °C to 95 °C as function of radiation dose ($E = 8.5$ keV). The empirically determined relation was T_g (°C) $\approx 118.0 - 8.0 \times 10^{-3} \varepsilon$ (mJ/mm³), where ε is the absorbed dose expressed in Gray units¹¹⁶. The maximum dose administered was about 2000 kGy. For comparison, it is noted that in industrial processing, doses in the range of 50 – 2000 kGy are within the normal range to transform semicrystalline thermoplasts to thermosets³⁹. Tools to perform cross correlations to assess the degree of cross linking can be ¹³C-NMR and photoelectron spectroscopy³⁹.

The lowering of the T_g can be seen as radiation damage, but was also shown to influence the coalescence behavior of PMMA colloids¹¹⁷ deposited onto Kapton films and imaged with 8 keV photons with a dose rate of 2×10^{11} ph/s and a beam size of 15×15 μm^2 . Coalescence generally requires elevated temperatures, but was observed to occur here upon radiation at ambient temperature. Further, when using different monodisperse samples (radii $R=100, 550, 1000$ and 1800 nm), it was found that smaller radii samples coalesced faster. The process resembled viscoelastic coalescence, but was not observed in non-irradiated materials. The authors attribute this effect to polymeric scission, which reduces the T_g , surface tension and viscosity of the colloids.

Chemical reactions that involve radicals are likely candidates for radiation-induced interference. This has indeed been observed in the polymerization-induced self-assembly of poly(stearyl methacrylate)–poly(benzyl methacrylate) (PSMA–PBzMA) diblock copolymer via reversible addition–fragmentation chain transfer (RAFT) dispersion polymerization¹¹⁸. SAXS experiments, designed to follow the reaction kinetics, showed a fourfold increased reaction rate compared to off-line experiments. This increase was explained by presence of radiation induced free radicals.

In protein solution scattering experiments radiation damage is recognized by the aggregation of proteins. It is less well known that for synthetic polymers similar effects can occur. An extensive study of the radiation induced aggregation of [6,6]-phenyl-C71-butyric acid methyl ester (PC71BM) in chlorobenzene

1
2
3 with and without addition of 1,8-diiodooctane indeed showed such aggregation effects, which were not
4 observed in parallel neutron scattering experiments on the same material. The effect was less when 1,8-
5 diiodooctane ($C_8H_{16}I_2$) was present. One would expect that with the presence of the heavier iodine, more
6 absorption and photoelectrons would be created. Alternatively, it could be that the iodine acts as electron
7 scavenger¹¹⁹.
8
9

10 While the aggregation described above is permanent, reversible effects have also been found in solutions
11 containing self-assembling stiff supramolecular peptide filaments¹²⁰. Here, when radiation is applied
12 during the growth phase, crystalline bundles are formed that then loose regular ordering when exposure
13 ceases. The changes of the surface charge density induced by radiolysis products are the likely cause. It is
14 noteworthy that the radiation has to be applied during the growth phase to observe this effect. This is
15 reminiscent of the orientation of bundles of stiff biological macromolecules grown under an applied force
16 field. Here, bundling should take place before the molecules are too long and steric hindering inhibits the
17 reorientation required for bundle formation^{121, 122}.
18
19

20 Dynamic events at the very local level, as measured by XPCS, can also be influenced by radiation. In
21 stretched elastomers, filled with either Si or carbon black, it was observed that the Si particle mobility was
22 reduced as function of the radiation dose. In this case, the authors speculated that radiation damage
23 caused crosslinking and hence a slowing down of the Si particles by the increase in stiffness of the polymer
24 network¹²³, but could not verify the same behavior for the carbon black filled sample. However, this
25 system is somewhat confusing. Experiments on samples of the same material swollen in a solvent using
26 an estimated 300-fold increase in incident flux, showed a breaking from the crosslinks which allowed the
27 Si particles to diffuse out of the beam¹²⁴. As these authors state: 'However, even if there is no obvious
28 change in the scattering intensity profiles, the dynamics suffer from the radiation damage as shown in this
29 study'. The real problem here, as noted before, lies in distinguishing the radiation induced effects from
30 the real physics. The uncertainty in interpretation of the results in the examples above illustrate the
31 difficulties of making accurate predictions of how polymeric materials will react to exposure to radiation.
32
33
34

35 ***3.5 Interference and radiochemistry in water and other solvents***

36
37

38 In the section on interfaces, several examples of metallic nanoparticle synthesis in irradiated solvents
39 were given with specific emphasis on how this could be used to produce coatings. It is thus interesting to
40 compare the radiation doses used in this type of manufacturing with the radiation doses used on
41 beamlines for characterization. For radiation induced/assisted polymerization of dissolved synthetic
42 polymers, values of an absorbed 30 kGy total dose with a dose rate of 1.8 kGy/hour have been reported¹²⁵.
43 Gel formation in polymer solutions is reported for 2 kGy total dose¹²⁶. A non-exhaustive survey of the
44 radiation induced formation of different metallic (colloidal Au, core shell bimetallic Cu-Al, etc.)
45 nanoparticles shows that, depending on the solvent conditions, dose rates 8 - 60 kGy/hour and total dose
46 of 40 – 250 kGy are being used¹²⁷⁻¹³⁰.
47
48
49

50 As comparison, consider the radiation dose on a modern microfocus synchrotron beamline. A water
51 sample of 2 mm thick will absorb approximately 70% of 10 keV photons. We assume that the absorption
52 is distributed evenly over the irradiated volume. Mounted on a microfocus beamline with a size of 10 x 10
53 μm^2 and 10^{13} photons/sec this sample receives 500 kGy/s, which is considerably higher than the doses
54
55
56
57
58
59
60

used in the industrial contexts. Mitigating circumstances will be that material can diffuse out of the volume exposed to the synchrotron beam. This, however, also indicates that viscosity can play a role.

In this context it is not surprising that in pink beam energy dispersive XAFS experiments⁴⁸, where the absorbed X-ray dose will again be considerably higher, it was found that the reaction rate of the oxidation of benzyl alcohol to benzaldehyde using a copper bipyridine (1:1) complex was considerably increased. See figure 10.

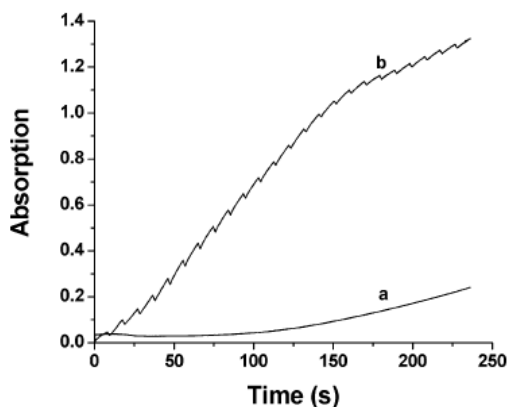


Figure 10

Uv-Vis intensity monitoring the advance of the conversion of benzyl alcohol to benzaldehyde as function of time. The bottom curve shows the intensity without X-ray irradiation. The top curve is when the sample is exposed to X-ray. The discontinuities are due to the periodic closure of the X-ray shutter. The increase in the reaction rate is clearly visible. Reprinted with permission⁴⁸

A further investigation on Cu salt solutions with different ligands but without the presence of a catalyst showed that the ligands could influence the rate at which the Cu ions were reduced^{48, 131}. These effects were observed on both polychromatic as well as monochromatic bending magnet beamlines, with differences of 0.38 kGy versus 41.5 kGy. Reduction of the Cu allowed the formation of 2-3 nm sized Cu nanoparticles, as well as the formation of gas bubbles. Gas formation in solutions has also been observed over a range of intensities in monochromatic beamline experiments, in solutions to which LiBr was added¹.

Similar experiments have followed the formation of Ag particles in a polymer/water/AgClO₄ solution. Here, X-ray experiments were performed after exposure of samples to a 500 W Mercury lamp¹³². The effects of the exposure to two different photon sources are difficult to disentangle.

While the examples above use polychromatic beams, it is clear that lower intensity monochromatic beams could induce the same effects over a longer time-scale⁴⁸. This is confirmed by the observation that Au nanoparticles form under the influence of a monochromatic irradiation¹¹². In contrast, however, the growth rate of Bi₂O₂CO₃ crystals from a solution was slowed down considerably under irradiation compared to off-line experiments¹³³. In this case, the growth process was shown to be pH dependent which could explain why the on- and off-line results differ.

With simple solutions containing a single additive, it is relatively simple to deduce which reaction(s) may occur upon exposure to X-rays. In a previous section, it was noted that the presence of an interface can complicate matters and this is also the case with more complex solutions in which different particles are

grafted to each other. An elaborate example can be found in the reduction of graphene oxide attached to TiO_2 particles in an acidic environment¹³⁴.

In low concentration solutions of long stiff supramolecular peptide filaments, it was observed that exposure to monochromatic X-rays (dose 4.4 kGy/s) induced the formation of highly ordered hexagonal bundles¹³⁵. Although the bundle formation was reversible, it was found that these bundles could remain stable for many hours after irradiation had ceased. Induced charges, rather than chemical crosslinking, was found to be the cause of the bundle formation. The stability of such bundles has also been observed in other rigid rod systems¹²¹ and is not necessarily related to irradiation, since steric hindering of the rotational diffusion should also be taken into account. At higher peptide concentrations the bundle formation was spontaneous, and irradiation played a minor role. See Figure 11.

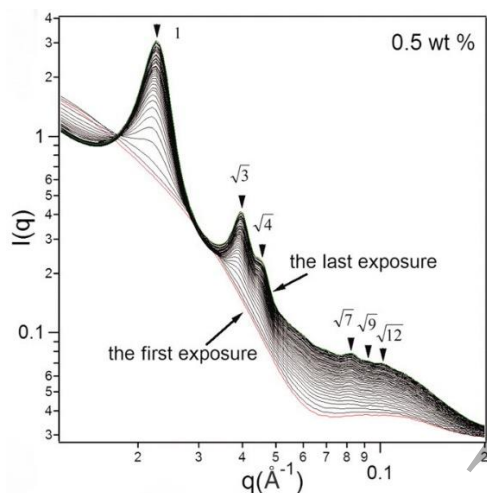


Figure 11

SAXS patterns of the formation of highly ordered structure by supramolecular peptide filaments upon irradiation. The bundle formation was reversible upon termination of the irradiation. (50 exposures of 4 seconds with a dose rate of dose 4.4 kGy/s). Reprinted with permission¹²⁰.

The rotation of ordered domains of microtubules towards the beam position in low viscosity Pipes buffers has also been found. (Bras, Diakun, Diaz unpublished data). This was not observed in higher viscosity glycerol containing buffer solutions.

If we consider for a moment how the numbers mentioned above compare to a modern X-ray source with a metal jet generator, 1 mm thick water or polymer sample, we find that samples on these instruments absorb about 2 Gy/s. A 15 minute experiment will therefore render a dose similar to that reported for the purposeful cross linking of polymer gels¹²⁶.

4. Conclusions

It is undeniable that the increases in X-ray photon flux produced by synchrotron radiation sources have enabled many previously impossible scientific experiments. A darker side to this development is the increased possibility of inflicting radiation damage. For some research areas, one may wonder if the limit

1
2
3 of what materials can handle has already been reached and whether it makes sense to increase beam
4 brilliance any further. But generally, radiation damage is recognizable and can frequently be addressed.

5
6 Other potential effects of increased brilliance, like structural or electronic modifications or the influence
7 that radiation can have on kinetic processes, are less recognized. This concerns experiments where the
8 sample remains in beam for extended periods of time, where one wants to study the evolution of sample
9 properties on time scales that are relevant for the physical/chemical process under consideration.

10
11 We have attempted here to raise awareness of some of the many effects which may arise, but have not
12 attempted to distill the radiation dose limits that specific materials can handle. This task is impossible and
13 has to be considered on a case-by-case basis. We have cited examples ranging from the induced
14 crystallization in lemon flavored Jelly-O, due to an X-ray beam generated by a sealed tube source, to the
15 particle formation in the high intensity beams of 3rd generation pink beam undulators. In order to better
16 understand and/or predict what may happen in a given sample, one could contemplate to utilize
17 modelling techniques. This has been reasonably successful, for example, in predicting damage thresholds
18 and limits in macromolecular crystallography. In cases where interfaces are present, and with more
19 complex sample compositions, the number of reactions and other compounding factors that may
20 influence a process is considerably larger, and it is doubtful if at present this could render reliable results
21 in individual cases, let alone to develop generally applicable methodology.

22
23 For the foreseeable future, one has to rely on empirical results and good experimental practices. The
24 advice to use the minimum radiation dose required to obtain the necessary data is obvious but often
25 forgotten. It is crucial to be aware of and monitor radiation sensitive parameters during the experiment
26 and to then examine cross correlations between materials that have undergone the same
27 physical/chemical treatment with and without exposure to X-rays.

28
29 Although X-ray damage is well known, the occurrence of inadvertent effects described in this paper should
30 serve as an extra reminder to machine and beam line developers (and their management and funding
31 agencies) that pursuit of ever-increasing brilliances is at times at odds with the radiation loads that
32 materials can withstand, and/or in generating additional effects that mask or complicate the scientific
33 questions at hand. The range and variety of radiation effects observed across differing materials
34 (spanning hard, soft, biological, synthetic, and composite materials and devices), and their likely less
35 frequently recognized influences in time-resolved experiments, urges caution and care in the design and
36 interpretation of such experiments. Clearly, while the constant upgrade of synchrotron sources demands
37 large financial commitment, investments also need to be made to advance methods and tools that can
38 help predict, mitigate and perhaps better control and exploit not only directly observed effects of
39 radiation damage, but also the less evident radiation-induced influences and effects on the structure,
40 properties and chemical states etc. of materials.

41
42 To end on a particularly positive note, one should maybe be reminded that in the 1970's, the initial
43 reaction of the protein crystallography community on the possibilities for use of synchrotron radiation
44 was tempered by the anticipated problems and concerns of radiation damage¹³⁶. It is fair to say that these
45 initial considerations were superseded by an enthusiastic embrace once methods had been found to
46 mitigate the damage and that protein research became one of the main drivers for further beam line and
47 storage ring development. This will be feasible in other branches of research as well, if we work on it now.

5. Acknowledgements

Oleg Mykhaylyk, Scott Barton, Karsten Joensen. Dirk Detollenaere, Ian Gillan (for 'Smoke on the Sample'), Stephan Förster, John Helliwell, Colin Nave and Sean McSweeney are thanked for their comments and contributions. Acknowledgements should also be given to the late Neville Greaves whom played throughout his career such an important role in the development of time resolved X-ray spectroscopy and X-ray scattering for materials science and catalysis applications.

W.B.'s and D.A.A.M's contribution is based upon work supported by Oak Ridge National Laboratory, managed by UT-Battelle LLC, for the U.S. Department of Energy.

6. References

1. Bras, W.; Stanley, H. *Journal of Non-Crystalline Solids* **2016**, 451, 153-160.
2. Hemberg, O.; Otendal, M.; Hertz, H. M. *Applied Physics Letters* **2003**, 83, (7), 1483-1485.
3. Hemberg, O.; Otendal, M.; Hertz, H. M. *Optical Engineering* **2004**, 43, (7), 1682-1688.
4. Skarzynski, T. *Acta Crystallographica Section D* **2013**, 69, (7), 1283-1288.
5. Susich, G.; King, A. O.; Dogliotti, L. M. *Science* **1959**, 130, (3375), 567-568.
6. Cho, G. L.; Ha, J. W. *Food Control* **2019**, 96, 343-350.
7. Choi, J. I.; Lim, S. *Radiation Physics and Chemistry* **2016**, 118, 70-74.
8. Breen, A. P.; Murphy, J. A. *Free Radical Biology and Medicine* **1995**, 18, (6), 1033-1077.
9. Fernandez, M. P.; Dall'Ara, E.; Kao, A. P.; Bodey, A. J.; Karali, A.; Blunn, G. W.; Barber, A. H.; Tozzi, G. *Materials* **2018**, 11, (11), 17.
10. Kozachuk, M.; Suda, A.; Ellis, L.; Walzak, M.; Biesinger, M.; Macfie, S.; Hudson, R.; Nelson, A.; Martin, R.; Heginbotham, A. *Journal of Conservation and Museum Studies* **2016**, 14, (1), 6.
11. Ravelli, R. B. G.; McSweeney, S. M. *Struct. Fold. Des.* **2000**, 8, (3), 315-328.
12. Schnabel, W., *Polymers and electromagnetic radiation*. Wiley: 2014.
13. Greaves, G. N. *Philosophical Magazine B* **1978**, 37, (4), 447-466.
14. Duraud, J. P.; Jollet, F.; Langevin, Y.; Dooryhee, E. *Nuclear Instruments and Methods in Physics Research Section B: Beam Interactions with Materials and Atoms* **1988**, 32, (1), 248-257.
15. Knoll, G. F., *Radiation detection and measurement*. 2nd ed.; John Wiley and Sons: 1989.
16. Leroy, C.; Rancoita, P., *Principles of Radiation Interaction in matter and detection*. 3rd ed.; World Scientific: 2012.
17. Henke, B. L.; Gullikson, E. M.; Davis, J. C. *Atomic Data and Nuclear Data Tables* **1993**, 54, (2), 181-342.
18. Shinotsuka, H.; Da, B.; Tanuma, S.; Yoshikawa, H.; Powell, C. J.; Penn, D. R. *Surface and Interface Analysis* **2017**, 49, (4), 238-252.
19. Nikjoo, H.; Uehara, S.; Emfietzoglou, D.; Brahme, A. *New Journal of Physics* **2008**, 10, 28.
20. Ziaja, B.; Szoke, A.; van der Spoel, D.; Hajdu, J. *Physical Review B* **2002**, 66, (2).
21. Ziaja, B.; London, R. A.; Hajdu, J. *Journal of Applied Physics* **2006**, 99, (3).
22. Lingerfelt, D. B.; Ganesh, P.; Jakowski, J.; Sumpter, B. G. *Journal of Chemical Theory and Computation* **2020**, 16, (2), 1200-1214.
23. Sanishvili, R.; Yoder, D. W.; Pothineni, S. B.; Rosenbaum, G.; Xu, S.; Vogt, S.; Stepanova, S.; Makarov, O. A.; Corcoran, S.; Benn, R.; Nagarajan, V.; Smith, J. L.; Fischetti, R. F. *Proceedings of the National Academy of Sciences of the United States of America* **2011**, 108, (15), 6127-6132.
24. Nicholson, J.; Nave, C.; Fayz, K.; Fell, B.; Garman, E. *Nuclear Instruments & Methods in Physics Research Section a-Accelerators Spectrometers Detectors and Associated Equipment* **2001**, 467, 1380-1383.
25. Kuzay, T. M.; Kazmierczak, M.; Hsieh, B. J. *Acta Crystallographica Section D-Biological Crystallography* **2001**, 57, 69-81.
26. Ponomarenko, O.; Nikulin, A. Y.; Moser, H. O.; Yang, P.; Sakata, O. *Journal of Synchrotron Radiation* **2011**, 18, 580-594.
27. Snell, E. H.; Bellamy, H. D.; Rosenbaum, G.; van der Woerd, M. J. *Journal Of Synchrotron Radiation* **2007**, 14, 109-115.
28. Warren, A. J.; Axford, D.; Owen, R. L. *Journal of Synchrotron Radiation* **2019**, 26, (4), 991-997.
29. Wallander, H.; Wallentin, J. *Journal of Synchrotron Radiation* **2017**, 24, 925-933.
30. Bonino, V.; Torsello, D.; Prestipino, C.; Mino, L.; Truccato, M. *Journal of Synchrotron Radiation* **2020**, 27, (6), 1662-1673.

- 1
2
3 31. Stanley, H. B.; Banerjee, D.; van Breemen, L.; Ciston, J.; Liebscher, C. H.; Martis, V.; Merino, D. H.;
4 Longo, A.; Pattison, P.; Peters, G. W. M.; Portale, G.; Sen, S.; Bras, W. *Crystengcomm* **2014**, 16, (39),
5 9331-9339.
6
7 32. Rosenthal, M.; Doblas, D.; Hernandez, J. J.; Odarchenko, Y. I.; Burghammer, M.; Di Cola, E.;
8 Spitzer, D.; Antipov, A. E.; Aldoshin, L. S.; Ivanov, D. A. *Journal Of Synchrotron Radiation* **2014**, 21, 223-
9 228.
10 33. Lexa, D.; Kropf, A. J. *Thermochimica Acta* **2003**, 401, (2), 239-242.
11 34. Chernyshov, D.; Dyadkin, V.; Bosak, A. *Phase Transit.* **2015**, 88, (3), 264-272.
12 35. Warren, N. J.; Mykhaylyk, O. O.; Mahmood, D.; Ryan, A. J.; Armes, S. P. *Journal of the American*
13 *Chemical Society* **2014**, 136, (3), 1023-1033.
14 36. Witala, M.; Han, J.; Menzel, A.; Nygard, K. *Journal of Applied Crystallography* **2014**, 47, 2078-
15 2080.
16 37. Han, Z. Y.; Li, S. H.; Tso, M. Y. W. *Radiation Effects and Defects in Solids* **2000**, 152, (4), 307-314.
17 38. Armistead, W. H.; Stookey, S. D. *Science* **1964**, 144, (361), 150-&.
18 39. Makuuchi, K.; Cheng, S., *Radiation Processing of polymer materials and its industrial*
20 *applications*. Wiley: 2012.
21 40. Przybytniak, G.; Sadlo, J.; Walo, M. *Express Polymer Letters* **2020**, 14, (6), 556-565.
22 41. Jahan, M. S.; Walters, B. M.; Riahinasab, T.; Gnawali, R.; Adhikari, D.; Trieu, H. *Radiation Physics*
23 *and Chemistry* **2016**, 118, 96-101.
24 42. Coffey, T.; Urquhart, S. G.; Ade, H. *Journal of Electron Spectroscopy and Related Phenomena*
25 **2002**, 122, (1), 65-78.
26 43. Bras, W.; Goossens, H.; Goderis, B. *IOP Conference Series: Materials Science and Engineering*,
27 012001 (14 pp.).
28 44. Swallow, A. J., *Radiation Chemistry of Organic Compounds*. Pergamon press: 1960.
29 45. Roots, R.; Okada, S. *Radiat. Res.* **1975**, 64, (2), 306-320.
30 46. Martis, V.; Nikitenko, S.; Sen, S.; Sankar, G.; van Beek, W.; Filinchuk, Y.; Snigireva, I.; Bras, W.
31 *Crystal Growth & Design* **2011**, 11, (7), 2858-2865.
32 47. Buxton, G., Radiation Chemistry From Basics to Applications in Material and Life Sciences. In *EDP*
33 *Sciences*, Spothem-Maurizot M.; Mostafavi M.; Douki T.; J, B., Eds. Courtaboeuf, 2008; pp 3-16.
34 48. Mesu, J. G.; van der Eerden, A. M. J.; de Groot, F. M. F.; Weckhuysen, B. M. *Journal Of Physical*
35 *Chemistry B* **2005**, 109, (9), 4042-4047.
36 49. Royall, C. P.; Thiel, B. L.; Donald, A. M. *Journal of Microscopy-Oxford* **2001**, 204, 185-195.
37 50. Abellan, P.; Woehl, T. J.; Parent, L. R.; Browning, N. D.; Evans, J. E.; Arslan, I. *Chemical*
38 *Communications* **2014**, 50, (38), 4873-4880.
39 51. Schneider, N. M.; Norton, M. M.; Mendel, B. J.; Grogan, J. M.; Ross, F. M.; Bau, H. H. *Journal of*
40 *Physical Chemistry C* **2014**, 118, (38), 22373-22382.
41 52. Marignier, J. L.; Belloni, J.; Delcourt, M. O.; Chevalier, J. P. *Nature* **1985**, 317, (6035), 344-345.
42 53. Belloni, J.; Marignier, J. L.; Mostafavi, M. *Radiation Physics and Chemistry* **2020**, 169, 107952.
43 54. Flores-Rojas, G. G.; López-Saucedo, F.; Bucio, E. *Radiation Physics and Chemistry* **2020**, 169,
44 107962.
45 55. Yamaguchi, A.; Sakurai, I.; Okada, I.; Izumi, H.; Ishihara, M.; Fukuoka, T.; Suzuki, S.; Utsumi, Y.
46 *Journal of Synchrotron Radiation* **2020**, 27, (4), 1008-1014.
47 56. Komsa, H.-P.; Kotakoski, J.; Kurasch, S.; Lehtinen, O.; Kaiser, U.; Krashenninnikov, A. V. *Physical*
48 *Review Letters* **2012**, 109, (3), 035503.
49 57. Wei, X.; Tang, D.-M.; Chen, Q.; Bando, Y.; Golberg, D. *ACS Nano* **2013**, 7, (4), 3491-3497.
50 58. Ugurlu, O.; Haus, J.; Gunawan, A. A.; Thomas, M. G.; Maheshwari, S.; Tsapatsis, M.; Mkhoyan, K.
51 *A. Physical Review B* **2011**, 83, (11), 113408.
52
53
54
55
56
57
58
59
60

- 1
2
3 59. Kotomin, E. A.; Popov, A. I. *Nuclear Instruments & Methods in Physics Research Section B-Beam Interactions with Materials and Atoms* **1998**, 141, (1-4), 1-15.
- 4
5 60. Kretschmer, S.; Lehnert, T.; Kaiser, U.; Krasheninnikov, A. V. *Nano Letters* **2020**, 20, (4), 2865-2870.
- 6
7 61. Popov, A. I.; Kotomin, E. A.; Maier, J. *Nuclear Instruments and Methods in Physics Research Section B: Beam Interactions with Materials and Atoms* **2010**, 268, (19), 3084-3089.
- 8
9 62. Moncke, D.; Reibstein, S.; Schumacher, D.; Wondraczek, L. *Journal of Non-Crystalline Solids* **2014**, 383, 33-37.
- 10
11 63. Chirila, M. M.; Garces, N. Y.; Halliburton, L. E.; Demos, S. G.; Land, T. A.; Radousky, H. B. *Journal of Applied Physics* **2003**, 94, (10), 6456-6462.
- 12
13 64. Sheng, J.; Zhang, J.; Qiao, L. *Journal of Non-Crystalline Solids* **2006**, 352, (26), 2914-2916.
- 14
15 65. Richards, G. D.; Jabbour, R. S.; Horton, C. F.; Ibarra, C. L.; MacDowell, A. A. *Am J Phys Anthropol* **2012**, 149, (2), 172-80.
- 16
17 66. Spurný, Z.; Novotný, J. *Journal of Physics and Chemistry of Solids* **1965**, 26, (7), 1107-1110.
- 18
19 67. Wherland, S.; Pecht, I. *Proteins-Structure Function and Bioinformatics* **2018**, 86, (8), 817-826.
- 20
21 68. Yano, J.; Kern, J.; Irrgang, K. D.; Latimer, M. J.; Bergmann, U.; Glatzel, P.; Pushkar, Y.; Biesiadka, J.; Loll, B.; Sauer, K.; Messinger, J.; Zouni, A.; Yachandra, V. K. *Proceedings of the National Academy of Sciences of the United States of America* **2005**, 102, (34), 12047-12052.
- 22
23 69. Bourhis, K.; Royon, A.; Papon, G.; Bellec, M.; Petit, Y.; Canioni, L.; Dussauze, M.; Rodriguez, V.; Binet, L.; Caurant, D.; Treguer, M.; Videau, J. J.; Cardinal, T. *Materials Research Bulletin* **2013**, 48, (4), 1637-1644.
- 24
25 70. Fujita, S., *Organic Chemistry of Photography*. Springer: 2004.
- 26
27 71. Chapman, H. N.; Fromme, P.; Barty, A.; White, T. A.; Kirian, R. A.; Aquila, A.; Hunter, M. S.; Schulz, J.; DePonte, D. P.; Weierstall, U.; Doak, R. B.; Maia, F.; Martin, A. V.; Schlichting, I.; Lomb, L.; Coppola, N.; Shoeman, R. L.; Epp, S. W.; Hartmann, R.; Rolles, D.; Rudenko, A.; Foucar, L.; Kimmel, N.; Weidenspointner, G.; Holl, P.; Liang, M. N.; Barthelmeß, M.; Caleman, C.; Boutet, S.; Bogan, M. J.; Krzywinski, J.; Bostedt, C.; Bajt, S.; Gumprecht, L.; Rudek, B.; Erk, B.; Schmidt, C.; Homke, A.; Reich, C.; Pietschner, D.; Struder, L.; Hauser, G.; Gorke, H.; Ullrich, J.; Herrmann, S.; Schaller, G.; Schopper, F.; Soltau, H.; Kuhnelt, K. U.; Messerschmidt, M.; Bozek, J. D.; Hau-Riege, S. P.; Frank, M.; Hampton, C. Y.; Sierra, R. G.; Starodub, D.; Williams, G. J.; Hajdu, J.; Timneanu, N.; Seibert, M. M.; Andreasson, J.; Rocker, A.; Jonsson, O.; Svenda, M.; Stern, S.; Nass, K.; Andritschke, R.; Schroter, C. D.; Krasniqi, F.; Bott, M.; Schmidt, K. E.; Wang, X. Y.; Grotjohann, I.; Holton, J. M.; Barends, T. R. M.; Neutze, R.; Marchesini, S.; Fromme, R.; Schorb, S.; Rupp, D.; Adolph, M.; Gorkhover, T.; Andersson, I.; Hirsemann, H.; Potdevin, G.; Graafsma, H.; Nilsson, B.; Spence, J. C. H. *Nature* **2011**, 470, (7332), 73-U81.
- 30
31 72. Garman, E. F.; Weik, M. *Journal of Synchrotron Radiation* **2013**, 20, 1-6.
- 32
33 73. Gonzalez, A.; Nave, C. *Acta Crystallographica Section D-Biological Crystallography* **1994**, 50, 874-877.
- 34
35 74. Weik, M.; Berges, J.; Raves, M. L.; Gros, P.; McSweeney, S.; Silman, I.; Sussman, J. L.; Houee-Levin, C.; Ravelli, R. B. G. *Journal of Synchrotron Radiation* **2002**, 9, (6), 342-346.
- 36
37 75. Weik, M.; Ravelli, R. B. G.; Kryger, G.; McSweeney, S.; Raves, M. L.; Harel, M.; Gros, P.; Silman, I.; Kroon, J.; Sussman, J. L. *Proceedings of the National Academy of Sciences* **2000**, 97, (2), 623-628.
- 38
39 76. Hough, M. A.; Antonyuk, S. V.; Strange, R. W.; Eady, R. R.; Hasnain, S. S. *Journal of Molecular Biology* **2008**, 378, (2), 353-361.
- 40
41 77. Kmetko, J.; Warkentin, M.; Englich, U.; Thorne, R. E. *Acta Crystallographica Section D* **2011**, 67, (10), 881-893.
- 42
43 78. Beitlich, T.; Kuhnelt, K.; Schulze-Briese, C.; Shoeman, R. L.; Schlichting, I. *Journal of Synchrotron Radiation* **2007**, 14, (1), 11-23.
- 44
45
46
47
48
49
50
51
52
53
54
55
56
57
58
59
60

- 1
2
3 79. Pfanzagl, V.; Beale, J. H.; Michlits, H.; Schmidt, D.; Gabler, T.; Obinger, C.; Djinović-Carugo, K.;
4 Hofbauer, S. *Journal of Biological Chemistry* **2020**, 295, (39), 13488-13501.
- 5 80. McEvoy, J. P.; Brudvig, G. W. *Chemical Reviews* **2006**, 106, (11), 4455-4483.
- 6 81. KOK, B.; FORBUSH, B.; McGLOIN, M. *Photochemistry and Photobiology* **1970**, 11, (6), 457-475.
- 7 82. Davis, K. M.; Mattern, B. A.; Pacold, J. I.; Zakharova, T.; Brewe, D.; Kosheleva, I.; Henning, R. W.;
8 Graber, T. J.; Heald, S. M.; Seidler, G. T.; Pushkar, Y. *The Journal of Physical Chemistry Letters* **2012**, 3,
9 (14), 1858-1864.
- 10 83. Grabolle, M.; Haumann, M.; Müller, C.; Liebisch, P.; Dau, H. *Journal of Biological Chemistry* **2006**,
11 281, (8), 4580-4588.
- 12 84. Yano, J.; Yachandra, V. K. *Inorganic Chemistry* **2008**, 47, (6), 1711-1726.
- 13 85. Schlichting, I.; Berendzen, J.; Chu, K.; Stock, A. M.; Maves, S. A.; Benson, D. E.; Sweet, R. M.;
14 Ringe, D.; Petsko, G. A.; Sligar, S. G. *Science* **2000**, 287, (5458), 1615-1622.
- 15 86. Sawai, H.; Sugimoto, H.; Kato, Y.; Asano, Y.; Shiro, Y.; Aono, S. *Journal of Biological Chemistry*
16 **2009**, 284, (46), 32089-32096.
- 17 87. Huang, Z.; Bartels, M.; Xu, R.; Osterhoff, M.; Kalbfleisch, S.; Sprung, M.; Suzuki, A.; Takahashi, Y.;
18 Blanton, T. N.; Salditt, T.; Miao, J. *Nat Mater* **2015**, advance online publication.
- 19 88. Duffort, V.; Caignaert, V.; Pralong, V.; Raveau, B.; Suchomel, M. R.; Mitchell, J. F. *Solid State*
20 *Communications* **2014**, 182, 22-25.
- 21 89. Frantz, J.; Tarus, J.; Nordlund, K.; Keinonen, J. *Physical Review B* **2001**, 64, (12).
- 22 90. Jencic, I.; Bench, M. W.; Robertson, I. M.; Kirk, M. A. *Journal of Applied Physics* **1995**, 78, (2),
23 974-982.
- 24 91. Feldman, Y.; Lyahovitskaya, V.; Leitus, G.; Lubomirsky, I.; Wachtel, E.; Bushuev, V. A.; Vaughan,
25 G.; Barkay, Z.; Rosenberg, Y. *Applied Physics Letters* **2009**, 95, (5), 3.
- 26 92. Coutino-Gonzalez, E.; Grandjean, D.; Roeffaers, M.; Kvashnina, K.; Fron, E.; Dieu, B.; De Cremer,
27 G.; Lievens, P.; Sels, B.; Hofkens, J. *Chem Commun (Camb)* **2014**, 50, (11), 1350-2.
- 28 93. Fuhrmann, S.; Schumacher, D.; Herbst, J.; Wondraczek, L. *Journal of Non-Crystalline Solids* **2014**,
29 401, 82-86.
- 30 94. Funke, K.; Banhatti, R. D.; Grabowski, P.; Nowinski, J.; Wrobel, W.; Dinnebier, R.; Magdysyuk, O.
31 *Solid State Ionics* **2015**, 271, 2-9.
- 32 95. Eichelbaum, M.; Rademann, K.; Muller, R.; Radtke, M.; Riesemeier, H.; Gorner, W. *Angewandte*
33 *Chemie-International Edition* **2005**, 44, (48), 7905-7909.
- 34 96. Tatchev, D.; Hoell, A.; Eichelbaum, M.; Rademann, K. *Physical Review Letters* **2011**, 106, (8),
35 085702.
- 36 97. Chayanun, L.; Otnes, G.; Troian, A.; Hammarberg, S.; Salomon, D.; Borgstrom, M. T.; Wallentin, J.
37 *Journal of Synchrotron Radiation* **2019**, 26, (1), 102-108.
- 38 98. Kiryukhin, V.; Casa, D.; Hill, J. P.; Keimer, B.; Vigliante, A.; Tomioka, Y.; Tokura, Y. *Nature* **1997**,
39 386, (6627), 813-815.
- 40 99. Casa, D.; Kiryukhin, V.; Saleh, O. A.; Keimer, B.; Hill, J. P.; Tomioka, Y.; Tokura, Y. *Europhysics*
41 *Letters* **1999**, 47, (1), 90-96.
- 42 100. Liao, X.; Jeong, A. R.; Wilks, R. G.; Wiesner, S.; Rusu, M.; Bar, M. *Journal of Electron Spectroscopy*
43 *and Related Phenomena* **2016**, 212, 50-55.
- 44 101. Chang, S. H.; Kim, J.; Phatak, C.; D'Aquila, K.; Kim, S. K.; Song, S. J.; Hwang, C. S.; Eastman, J. A.;
45 Freeland, J. W.; Hong, S. *Acs Nano* **2014**, 8, (2), 1584-1589.
- 46 102. Pagliero, A.; Mino, L.; Borfecchia, E.; Truccato, M.; Agostino, A.; Pascale, L.; Enrico, E.; Leo, N. D.;
47 Lamberti, C.; Martínez-Criado, G. *Nano Letters* **2014**, 14, (3), 1583-1589.
- 48 103. Chushkin, Y. *Journal of Synchrotron Radiation* **2020**, 27, (5), 1247-1252.
- 49 104. Ruta, B.; Zontone, F.; Chushkin, Y.; Baldi, G.; Pintori, G.; Monaco, G.; Rufflé, B.; Kob, W. *Scientific*
50 *Reports* **2017**, 7, (1), 3962.
- 51
52
53
54
55
56
57
58
59
60

- 1
2
3 105. Schmalzried, H., *Chemical Kinetics of Solids*. VCH: 1995.
- 4 106. Newton, M. A.; Knorpp, A. J.; Meyet, J.; Stoian, D.; Nachtegaal, M.; Clark, A. H.; Safonova, O. V.;
5 Emerich, H.; van Beek, W.; Sushkevich, V. L.; van Bokhoven, J. A. *Physical Chemistry Chemical Physics*
6 **2020**.
- 7 107. Guilera, G.; Newton, M. A.; Polli, C.; Pascarelli, S.; Guino, M.; Hii, K. K. *Chemical Communications*
8 **2006**, (41), 4306-4308.
- 9 108. Hsu, P. C.; Wang, C. H.; Yang, T. Y.; Hwu, Y. K.; Lin, C. S.; Chen, C. H.; Chang, L. W.; Seol, S. K.; Je,
10 J. H.; Margaritondo, G. *J. Vac. Sci. Technol. A* **2007**, 25, (3), 615-620.
- 11 109. Hsu, P.-C.; Chen, Y.-S.; Hwu, Y.; Je, J. H.; Margaritondo, G.; Tok, E. S. *Journal of Synchrotron*
12 *Radiation* **2015**, 22, (6), 1524-1527.
- 13 110. Mesu, J. G., A M Beale, F M F de Groot; Weckhuysen, B. M. *J. Of Phys. Chem.* **2006**, 110, (35),
14 17671.
- 15 111. Clifford, D. M.; Castano, C. E.; Rojas, J. V. *Radiation Physics and Chemistry* **2018**, 144, 111-115.
- 16 112. Plech, A.; Kotaidis, V.; Siems, A.; Sztucki, M. *Physical Chemistry Chemical Physics* **2008**, 10, (26),
17 3888-3894.
- 18 113. Fraxedas, J.; Zhang, K.; Sepulveda, B.; Esplandiu, M. J.; de Andres, X. G.; Llorca, J.; Perez-Dieste,
19 V.; Escudero, C. *Journal of Synchrotron Radiation* **2019**, 26, 1288-1293.
- 20 114. Laanait, N.; Callagon, E. B. R.; Zhang, Z.; Sturchio, N. C.; Lee, S. S.; Fenter, P. *Science* **2015**, 349,
21 (6254), 1330-1334.
- 22 115. Weon, B. M.; Lee, J. S.; Je, J. H.; Fezzaa, K. *Physical Review E* **2011**, 84, (3).
- 23 116. Keymeulen, H. R.; Diaz, A.; Solak, H. H.; David, C.; Pfeiffer, F.; Patterson, B. D.; van der Veen, J. F.;
24 Stoykovich, M. P.; Nealey, P. F. *Journal Of Applied Physics* **2007**, 102, (1).
- 25 117. Weon, B. M.; Kim, J. T.; Je, J. H.; Yi, J. M.; Wang, S.; Lee, W. K. *Physical Review Letters* **2011**, 107,
26 (1), 018301.
- 27 118. Derry, M. J.; Fielding, L. A.; Warren, N. J.; Mable, C. J.; Smith, A. J.; Mykhaylyk, O. O.; Armes, S. P.
28 *Chemical Science* **2016**, 7, (8), 5078-5090.
- 29 119. Bernardo, G.; Washington, A. L.; Zhang, Y. W.; King, S. M.; Toolan, D. T. W.; Weir, M. P.; Dunbar,
30 A. D. F.; Howse, J. R.; Dattani, R.; Fairclough, J. P. A.; Parnell, A. J. *Royal Society Open Science* **2018**, 5, (9),
31 11.
- 32 120. Cui, H. G.; Pashuck, E. T.; Velichko, Y. S.; Weigand, S. J.; Cheetham, A. G.; Newcomb, C. J.; Stupp,
33 S. I. *Science* **2010**, 327, (5965), 555-559.
- 34 121. Bras, W.; Diakun, G. P.; Diaz, J. F.; Maret, G.; Kramer, H.; Bordas, J.; Medrano, F. J. *Biophysical*
35 *Journal* **1998**, 74, (3), 1509-1521.
- 36 122. Torbet, J.; Freyssinet, J. M.; Hudryclergeon, G. *Nature* **1981**, 289, (5793), 91-93.
- 37 123. Ehrburger-Dolle, F.; Morfin, I.; Bley, F.; Livet, F.; Heinrich, G.; Richter, S.; Piché, L.; Sutton, M.
38 *Macromolecules* **2012**, 45, (21), 8691-8701.
- 39 124. Shinohara, Y.; Yamamoto, N.; Kishimoto, H.; Amemiya, Y. *Journal of Synchrotron Radiation* **2015**,
40 22, 119-123.
- 41 125. Li, Q.; Fan, W.; Yang, T.; Wang, J.; Hu, L.; He, W.; Wen, W.; Liu, H. *Radiation Physics and*
42 *Chemistry* **2020**, 169, 107904.
- 43 126. Matusiak, M.; Kadlubowski, S.; Rosiak, J. M. *Radiation Physics and Chemistry* **2020**, 169, 108099.
- 44 127. Zezin, A. A.; Klimov, D. I.; Zezina, E. A.; Mkrtchyan, K. V.; Feldman, V. I. *Radiation Physics and*
45 *Chemistry* **2020**, 169, 108076.
- 46 128. Flores-Rojas, G. G.; Lopez-Saucedo, F.; Bucio, E. *Radiation Physics and Chemistry* **2020**, 169, 16.
- 47 129. Hanzic, N.; Jurkin, T.; Maksimovic, A.; Gotic, M. *Radiation Physics and Chemistry* **2015**, 106, 77-
48 82.
- 49 130. Larki, F.; Abedini, A.; Islam, M. S.; Shaari, S.; Ali, S. H. M.; Menon, P. S.; Jalar, A.; Saion, E.; Sampe,
50 J.; Majlis, B. Y. *Journal of Materials Science* **2015**, 50, (12), 4348-4356.
- 51
52
53
54
55
56
57
58
59
60

- 1
2
3 131. Mesu, J. G.; Beale, A. M.; de Groot, F. M. F.; Weckhuysen, B. M. *Journal Of Physical Chemistry B*
4 **2006**, 110, (35), 17671-17677.
5 132. Harada, M.; Inada, Y.; Nomura, M. *Journal of Colloid and Interface Science* **2009**, 337, (2), 427-
6 438.
7 133. More, R.; Olah, M.; Balaghi, S. E.; Jaker, P.; Siol, S.; Zhou, Y.; Patzke, G. R. *Acs Omega* **2017**, 2,
8 (11), 8213-8221.
9 134. Behar, D.; Rajh, T.; Liu, Y.; Connell, J.; Stamenkovic, V.; Rabani, J. *The Journal of Physical*
10 *Chemistry C* **2020**, 124, (9), 5425-5435.
11 135. Adamovsky, S.; Schick, C. *Thermochimica Acta* **2004**, 415, (1-2), 1-7.
12 136. Helliwell, J. R. *Crystallography Reviews* **2012**, 18, (1), 33-93.
13
14
15
16
17
18
19
20
21
22
23
24
25
26
27
28
29
30
31
32
33
34
35
36
37
38
39
40
41
42
43
44
45
46
47
48
49
50
51
52
53
54
55
56
57
58
59
60